

LEARNING A DENSE REASONING REWARD MODEL FROM EXPERT DEMONSTRATION VIA INVERSE REINFORCEMENT LEARNING

Claudio Fanconi
University of Cambridge
caf83@cam.ac.uk

Nicolás Astorga
University of Cambridge
nja46@cam.ac.uk

Mihaela van der Schaar
University of Cambridge
mv472@cam.ac.uk

ABSTRACT

We reframe and operationalise adversarial inverse reinforcement learning (IRL) to large language model reasoning, learning a dense, token-level reward model for process supervision directly from expert demonstrations rather than imitating style via supervised fine-tuning. The learned reasoning reward serves two complementary roles: (i) it provides step-level feedback to optimise a reasoning policy during training; and (ii) it functions at inference as a critic to rerank sampled traces under fixed compute budgets. We demonstrate that our approach prioritises correctness over surface form, yielding scores that correlate with eventual answer validity and enabling interpretable localisation of errors within a trace. Empirically, on GSM8K with Llama3 and Qwen2.5 backbones, we demonstrate: (i) dense reasoning rewards can be used as a learning signal to elicit reasoning, and (ii) predictive performance is improved from reward-guided reranking (notably for Llama-based policies). By unifying training signals, inference-time selection, and token-level diagnostics into a single reasoning reward, this work suggests reusable process-level rewards with broad potential to enhance multi-step reasoning in language models.¹

1 INTRODUCTION

Recent advancements in large language models (LLMs) have driven rapid progress on multi-step reasoning tasks. A dominant method is to transfer reasoning behaviours from human experts or stronger models via supervised fine-tuning (SFT) on their reasoning traces (DeepSeek-AI et al., 2025). While effective, this strategy fundamentally trains models to imitate a teacher’s style, rather than to optimise reasoning as a decision-making process. Moreover, pure imitation omits the exploration–exploitation trade-off that underpins autonomous improvement in sequential decision-making (Setlur et al., 2025).

We take a different route: we formulate process-level reasoning as an inverse reinforcement learning (IRL) problem. Instead of behaviour cloning from teacher LLMs (Sun and Schaar, 2025), we learn a dense reasoning reward model from expert demonstrations. This reasoning reward model evaluates intermediate steps within a reasoning trace and supplies token-wise feedback used in two complementary ways: (i) as a training signal to optimise a policy for reasoning, and (ii) at inference time, as an assistive reranker to select higher-quality samples under a fixed budget. In contrast to behaviour cloning, this IRL-based approach aims to encode principles of expert reasoning and to expose where a trace deviates from a good path through interpretable, dense rewards.

Defining a faithful, scalable, dense reward for reasoning is non-trivial: hand-crafted signals are task-specific, and often incentivise shortcuts. By contrast, expert reasoning traces are comparatively easier to collect at scale than carefully engineered token-level reward functions, and they implicitly contain information about which intermediate steps matter. We therefore learn the dense reward from expert demonstrations, rather than prescribing it, and use it for both training and inference-time assistance.

¹We provide the code for our experiments at https://github.com/fanconic/expert_reasoning

- We centre our formulation around four desiderata, evaluated empirically in this work:
1. **(D1) A reward model usable to train reasoning in an LLM.** Training with only outcome correctness lacks step-level guidance and encourages shortcut learning. Our learned reasoning reward model provides dense, token-level rewards that serve as a training signal for policy optimisation.
 2. **(D2) An inference-time assist to improve predictive performance.** In deployment we often have a small sampling budget; reranking or filtering can yield significant gains without retraining. We use the reasoning reward model to score and rerank sampled traces under a fixed budget.
 3. **(D3) Reward prefers being more likely correct, not only matching expert style.** Style imitation can embed biases and does not guarantee correctness. We show that the reasoning reward scores correlate positively with eventual correctness, rather than just surface form.
 4. **(D4) Interpretable dense reward that localises errors.** Process supervision should enable auditing and targeted intervention. We demonstrate how our reasoning reward model highlights erroneous steps within a trace, exposing where and how the reasoning deviates from the correct course.

We explicitly separate capability from predictive performance supremacy. Jointly optimising a policy with a learned process reward model realises the four desiderata above: (D1) a usable training signal, (D2) inference-time gains via reward-guided reranking under tight sampling budgets, (D3) rewards that favour likely-correct traces over mere stylistic conformity, and (D4) token-level diagnostics. Our main results centre on these capabilities—showing dense, token-level supervision, improved predictive performance via reward-guided selection, and interpretable error localisation.

A systematic overview of our method to learn a dense reasoning reward model is shown in Figure 1.

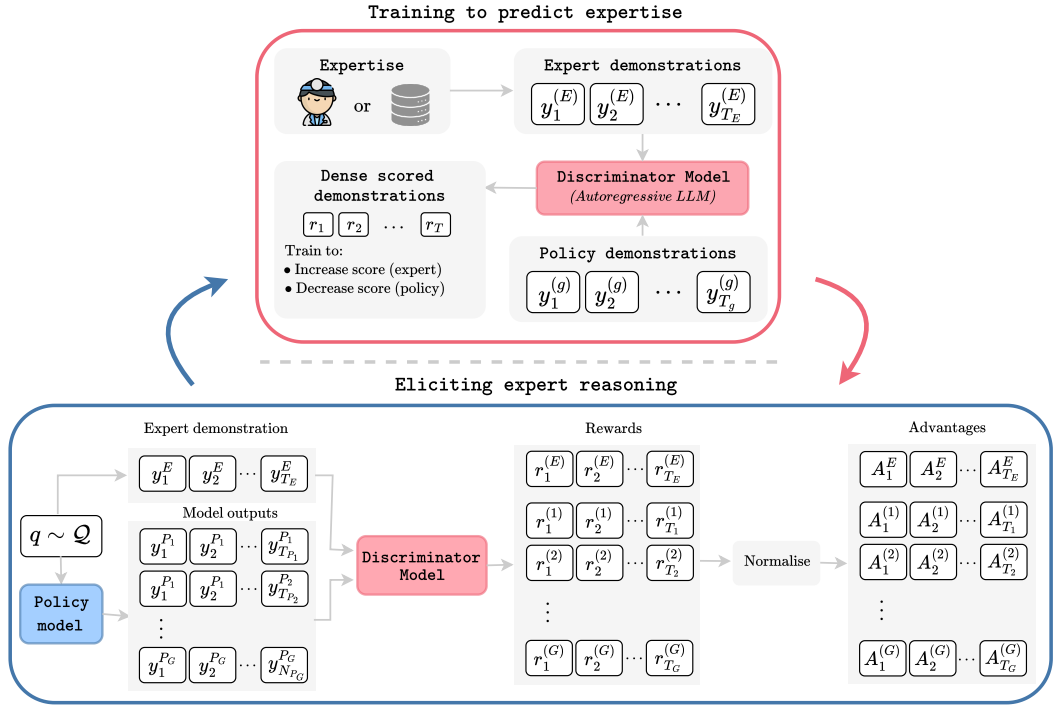


Figure 1: **Eliciting expert reasoning via adversarial inverse reinforcement learning.** The model learns a reasoning reward function from expert demonstrations using adversarial IRL.

2 RELATED WORK

Reinforcement Learning and Search for Reasoning. There is growing interest in using reinforcement learning (RL) to equip language models with improved reasoning by framing it as a sequential decision-making problem. Process supervision leverages process reward models (PRMs) to score intermediate steps rather than only final answers (DeepSeek-AI et al., 2025). This has been used to guide models in maths and logic by rewarding stepwise correctness (Uesato et al., 2022; Lightman et al., 2023), encouraging human-like solution paths in principle. However, specifying faithful, fine-grained rewards is non-trivial, and training separate PRMs invites reward hacking and additional complexity. Search-based approaches such as Monte Carlo Tree Search (MCTS) explore multiple reasoning paths and assign credit to steps that culminate in correct solutions (Zelikman et al., 2022; Yuan et al., 2023; Singh et al., 2024; Hosseini et al., 2024), echoing successes in games (Silver et al., 2017). Yet scaling MCTS to language is difficult due to the vast branching factor and noisy valuation of partial solutions. Closer to our aims, Cui et al. (2025) seeks to learn dense reasoning rewards via implicit rewards (Rafailov et al., 2024) and outcome-verifiable signals. Our work differs in that we learn a dense, token-level reward from expert demonstrations and utilise it both as a training signal and as an inference-time reranker.

Inverse Reinforcement Learning for LLM Alignment. Inverse reinforcement learning (IRL) infers a reward function from demonstrations rather than assuming it is known (Ziebart et al., 2004; Abbeel and Ng, 2004; Hejna and Sadigh, 2023; Fu et al., 2019; Ho and Ermon, 2016). This is attractive for aligning LLMs with human preferences and complex reasoning objectives that are difficult to specify, such as those used in RL with human feedback (RLHF) with preference data (Christiano et al., 2023; Rafailov et al., 2024). Recent works formalise alignment for language models as sequential decision-making with missing rewards (Sun and van der Schaar, 2024; Xia et al., 2024; Sun and van der Schaar, 2025), inferring rewards from high-quality trajectories (human experts or reliable AIs) to guide behaviour (Joselowitz et al., 2024). In traditional IRL literature, adversarial IRL methods train a discriminator to separate expert from generated traces and convert it into a reward (Ho and Ermon, 2016; Fu et al., 2018; Lin and Zhang, 2018; Li et al., 2017). We take this adversarial IRL perspective to learn a dense process-level critic from expert reasoning traces. This directly supports (D1) by providing a usable training signal, (D2) via inference-time reranking using the same critic, (D3) by favouring likely-correct traces rather than stylistic conformity, and (D4) by yielding token-level diagnostics.

Distillation and Supervised Fine-Tuning of Reasoning. A direct path to training reasoning models is supervised learning on demonstrations or rationales, often framed as knowledge distillation (Hinton et al., 2015). High-quality traces, from humans or strong teacher models, can be imitated to improve reasoning (DeepSeek-AI et al., 2025; Kang et al., 2023; Kujanpää et al., 2025; Xu et al., 2025). While SFT with chain-of-thought improves performance without RL’s optimisation challenges, pure imitation cannot explore or correct out-of-distribution states (Setlur et al., 2025). In our evaluation, SFT serves as a strong baseline for predictive performance. In contrast, our IRL-based approach prioritises capabilities: a reusable dense reward for training (D1), inference-time gains via reranking (D2), correctness-oriented scoring (D3), and interpretable token-level diagnostics (D4).

We summarise methodological differences with an emphasis on our desiderata in Table 1. The comparison highlights which approaches (i) learn a reward, (ii) provide dense, step-level signals, (iii) use expert demonstrations, (iv) naturally support inference-time assist (reranking/selection), and (v) generalise beyond stylistic imitation.

3 PROBLEM FORMALISM

We model reasoning as an autoregressive, sequential decision-making process. Given a prompt x , at step t the system is in state $s_t = (x, y_{<t})$ with $y_{<t} = (y_1, \dots, y_{t-1})$. The action space coincides with the vocabulary \mathcal{V} ; an action is the next token $y_t \in \mathcal{V}$. An output (reasoning trace) is a trajectory $\tau = (y_{1:T})$ of length T . The LLM, parameterised by θ , induces a policy

$$\pi_\theta(a_t | s_t) = \pi_\theta(y_t | x, y_{<t}),$$

and thereby a trajectory distribution $p_\theta(\tau | x)$ over \mathcal{T} , the space of token sequences. We write $x \sim \mathcal{Q}$ for the prompt distribution and $\tau_\theta \sim p_\theta(\cdot | x)$ for trajectories sampled from the current policy.

Method	Examples	Optimisation Objective	Learned Reward	Dense	Uses Experts	Inference Assist	Generalise beyond Style
SFT	DeepSeek-AI et al. (2025) Setlur et al. (2025) Kang et al. (2023)	$\max_{\theta} \mathbb{E}_{(x,y) \sim \mathcal{D}} [-\sum_t \log p_{\theta}(y_t x, y_{<t})]$	✗	✗	✓	✗	✗
Outcome Sup.	DeepSeek-AI et al. (2025)	$\max_{\theta} \mathbb{E}_{\tau \sim \pi_{\theta}} [r_{\text{out}}(\tau)]$	✗	✗	✗	✓	✓
Process-Sup.	Uesato et al. (2022) Lightman et al. (2023) Singh et al. (2024) Hosseini et al. (2024)	$\max_{\theta} \mathbb{E}_{\tau \sim \pi_{\theta}} [\sum_t r_{\text{proc}}(y_t)]$	✗	✓	✗	✓	✓
RLHF	Christiano et al. (2023)	$\max_{\theta} \mathbb{E}_{\tau \sim \pi_{\theta}} [\sum_t r_{\phi}(y_t)]$	✓	(✗)	(✓)	✓	✓
Expert Reas.	ours	$\max_{\phi} \min_{\theta} (\mathbb{E}_{\tau_E \sim p_E} [r_{\phi}(\tau_E)] - \mathbb{E}_{\tau_{\theta} \sim p_{\theta}} [r_{\phi}(\tau_{\theta})])$	✓	✓	✓	✓	✓

Table 1: **Comparison against desiderata.** Columns indicate whether a method (i) learns a reward, (ii) provides dense step-level signals (D1/D4), (iii) leverages expert demonstrations, (iv) naturally supports inference-time assistance via scoring/reranking (D2), and (v) facilitates generalisation beyond stylistic imitation towards correctness (D3).

Our goal is to learn π_{θ} that generates trajectories exhibiting high-quality chain-of-thought reasoning before answering. Unlike classical RL, an explicit reward is not observed: the latent evaluation function $r : \mathcal{T} \rightarrow \mathbb{R}$ (or token-level $r : \mathcal{S} \times \mathcal{V} \rightarrow \mathbb{R}$) is unknown. Instead, we assume access to expert demonstrations $\mathcal{D}_E = \{\tau_i^E\}_{i=1}^N$ drawn from an expert distribution $p_E(\tau | x)$, where each τ_i^E is a high-quality reasoning trace produced by a human expert or a stronger teacher model. The learning problem is to use \mathcal{D}_E to infer the structure of effective reasoning and to optimise π_{θ} so that $p_{\theta}(\cdot | x)$ aligns with $p_E(\cdot | x)$ while solving the underlying tasks.

To bridge to our IRL formulation, we introduce a parametric surrogate reward $r_{\phi} : \mathcal{T} \rightarrow \mathbb{R}$. The generic adversarial IRL objective seeks a saddle point in which the reward parameters ϕ maximise the separation between expert and policy trajectories while the policy parameters θ minimise it:

$$\max_{\phi} \min_{\theta} \mathbb{E}_{x \sim \mathcal{Q}} \left[\mathbb{E}_{\tau_E \sim p_E(\cdot | x)} [r_{\phi}(\tau_E)] - \mathbb{E}_{\tau_{\theta} \sim p_{\theta}(\cdot | x)} [r_{\phi}(\tau_{\theta})] \right]. \quad (1)$$

This objective formalises the goal: learn r_{ϕ} that scores expert reasoning higher than policy reasoning, while updating π_{θ} to close this gap.

4 METHOD

We build on adversarial learning frameworks for inverse reinforcement learning (Fu et al., 2018; Ho and Ermon, 2016), adapting them to the large-scale language modelling setting. While alternative IRL methods often rely on nested optimisation loops between policy and reward, making them computationally prohibitive for LLMs, adversarial training provides a more tractable approach with close parallels to RLHF (Sun and van der Schaar, 2025). Our method jointly learns a reward model for reasoning and optimises the LLM policy against it, moving beyond standard supervised fine-tuning. Figure 1 summarises the approach: a discriminator LLM is trained as an implicit reward model via adversarial learning, and the reasoning policy is updated using the induced dense rewards.

4.1 ADVERSARIAL LEARNING OF THE REASONING REWARD MODEL

Let an output (reasoning trace) be $\tau = (y_{1:T})$ with tokens $y_t \in \mathcal{V}$. We denote by p_E the distribution over expert outputs and by p_{θ} the distribution over outputs induced by the current LLM policy π_{θ} . Inspired by GAIL (Ho and Ermon, 2016) and AIRL (Fu et al., 2018), we train a discriminator LLM D_{ϕ} (parameters ϕ) to distinguish expert from policy-generated outputs: $D_{\phi}(\tau) \in [0, 1]$ is the probability that τ came from p_E rather than p_{θ} . The discriminator is trained with the standard binary cross-entropy objective

$$\max_{\phi} \mathcal{L}_D(\phi) = \mathbb{E}_{\tau \sim p_E} [\log D_{\phi}(\tau)] + \mathbb{E}_{\tau \sim p_{\theta}} [\log (1 - D_{\phi}(\tau))]. \quad (2)$$

For fixed p_{θ} , the optimal discriminator is (Goodfellow et al., 2014)

$$D_{\phi}^*(\tau) = \frac{p_E(\tau | x)}{p_E(\tau | x) + p_{\theta}(\tau | x)}, \quad (3)$$

which realises a density-ratio estimator between expert and policy distributions. Subsequently, we use the logit of the discriminator as an implicit reward to train the LLM reasoning policy τ_θ . In particular, at token position t with state $s_t = (x, y_{<t})$ and action y_t ,

$$r_\phi(s_t, y_t) = r_\phi(y_t | x, y_{<t}) = \log D_\phi(y_t | x, y_{<t}) - \log(1 - D_\phi(y_t | x, y_{<t})), \quad (4)$$

yielding dense, token-level process feedback without explicit human reward annotation. For simplicity of notation, we will omit the condition in the reward and discriminator, and refer to it as $r_\phi(y_t)$ and $D_\phi(y_t)$, respectively.

4.2 POLICY LEARNING WITH DENSE REASONING REWARDS

Let $x \sim \mathcal{Q}$ denote a prompt drawn from the prompt distribution. For each x , we form a per-prompt group consisting of one expert demonstration $\tau^E \sim p_E(\cdot | x)$ (if available) and G policy candidates $\{\tau^{(g)}\}_{g=1}^G \sim p_{\theta_{\text{old}}}(\cdot | x)$, where $\tau^{(g)} = (y_{1:T_g}^{(g)})$. Applying (4) gives token-level rewards $r_\phi(y_t^{(g)}) \in \mathbb{R}$ for each sequence in the group.

To reduce variance and remove scale dependence, we normalise each reward within the group for prompt x . For any sequence τ in the group, define the baseline as the average reward of the last valid token in the sequence, as it encapsulates the information of the previous prompt and response tokens. Subsequently, we divide by the standard deviation of the rewards of the last valid token.

Let $\mathcal{S} = \{\tau^E\} \cup \{\tau^{(g)}\}_{g=1}^G$. Compute the standardisation as proposed for Group Relative Policy Optimisation (GRPO) by Zhao et al. (2024):

$$\bar{r} = \frac{1}{|\mathcal{S}|} \sum_{\tau \in \mathcal{S}_x} r_\phi(y_{T_\tau}), \quad \sigma^2 = \frac{1}{|\mathcal{S}| - 1} \sum_{\tau \in \mathcal{S}} (r_\phi(y_{T_\tau}) - \bar{r})^2$$

Standardised individual token rewards are $\tilde{r}_\phi(y_t) = (r_\phi(y_t) - \bar{r})/\sigma$. Following the method proposed by Cui et al. (2025) for dense rewards, we define discounted advantages for each position t in a policy output $\tau^{(g)}$ as

$$A_t^{(g)} = \sum_{s=t}^{T_g} \gamma^{s-t} \tilde{r}_\phi(y_s^{(g)}), \quad \gamma \in [0, 1]. \quad (5)$$

For completeness, the same construction yields A_t^E on the expert trace, and the policy updates uses $\{A_t^{(g)}\}_{g=1}^G$ and A_t^E , which can be seen as a weak form of supervised-finetuning, as the expert demonstration is anyways available. Once all the advantages A_t for every token are calculated, we update the policy with the Proximal Policy Optimisation clip surrogate loss (Schulman et al., 2017):

$$\min_{\theta} \mathcal{L}_{\text{clip}}(\theta) = \mathbb{E}_t \left[\min \left(\frac{\pi_\theta(y_t | x, y_{<t})}{\pi_{\theta_{\text{old}}}(y_t | x, y_{<t})} A_t, \text{clip} \left(\frac{\pi_\theta(y_t | x, y_{<t})}{\pi_{\theta_{\text{old}}}(y_t | x, y_{<t})}, 1 - \epsilon, 1 + \epsilon \right) A_t \right) \right] \quad (6)$$

An overview of the training can be found in Algorithm 1.

Algorithm 1 Adversarial inverse reinforcement learning for eliciting expert reasoning in LLMs

Require: Expert reasoning traces $\mathcal{D}_E = \{\tau_i^E\}_{i=1}^N$; number of iterations I

- 1: Initialise reasoning policy π_θ and discriminator D_ϕ
 - 2: **for** $i \leftarrow 1$ to I **do**
 - 3: Generate G reasoning traces $\mathcal{D}_P \leftarrow \{\tau^{(g)}\}_{g=1}^G$ by sampling π_θ on prompts $x \sim \mathcal{Q}$
 - 4: (Optional) Add perturbed examples to \mathcal{D}_P
 - 5: Update D_ϕ : maximise $\mathbb{E}_{\tau \sim \mathcal{D}_E} [\log D_\phi(\tau)] + \mathbb{E}_{\tau \sim \mathcal{D}_P} [\log(1 - D_\phi(\tau))]$
 - 6: Compute reward for each token in \mathcal{S} : $r_\phi(y_t^{(g)}) \leftarrow \log(D_\phi(y_t^{(g)})) - \log(1 - D_\phi(y_t^{(g)}))$
 - 7: Normalise each reward $\tilde{r}_\phi(y_t^{(g)})$ and compute advantage score $A_t^{(g)}$
 - 8: Optimise π_θ by applying one step of GRPO on \mathcal{D}_ϕ using rewards r_ϕ
 - 9: **end for**
-

5 EXPERIMENTS

We evaluate on GSM8K (Cobbe et al., 2021), which includes human-annotated intermediate reasoning steps. Our base policies are open-weight, instruction-tuned variants not trained for reasoning: Qwen2.5 (policies: 3B, 7B; discriminators: 0.5B, 1.5B; Bai et al. (2023)) and Llama3 (policies: 3B, 8B; discriminator: 1B; Touvron et al. (2023)). Across different policy–discriminator pairings, we learn a dense, token-level reasoning reward from expert demonstrations and jointly optimise the policy with this reward. Evaluation follows the four desiderata from §1: (D1) reward as a training signal; (D2) inference-time assistance via critic-guided reranking under fixed sampling budgets; (D3) favouring likely-correct traces over stylistic conformity; and (D4) interpretable token-level diagnostics that localise errors. Implementation and optimisation details appear in Appendix A.

5.1 USING THE LEARNED REWARD AS A TRAINING SIGNAL

We first test whether the learned dense reasoning reward provides a useful signal for optimising a policy’s step wise behaviour. We jointly train a policy and dense reasoning reward model on GSM8K and monitor (i) the mean reward assigned to full traces on evaluation data and (ii) the fraction of traces that end in a correct answer (“correctness accuracy”) for both training and evaluation splits. Figure 2 shows the training dynamics for Llama3.1-8B with a Llama3.2-1B discriminator. The evaluation reward fluctuates from negative values toward zero and above, reflecting the adversarial interaction between the policy and the discriminator. The correctness accuracy increases, especially when the reward rises, and ends higher than before training.

We observe the same qualitative pattern across other policy and discriminator pairings, namely Qwen2.5 3B and 7B and Llama3 3B configurations, reported in Appendix B.1 Figures 7, 8, and 9. The evaluation reward tracks learning progress and is positively associated with correctness. This indicates that the discriminator’s token-level supervision is not only fitting training data but also generalises as a process signal.

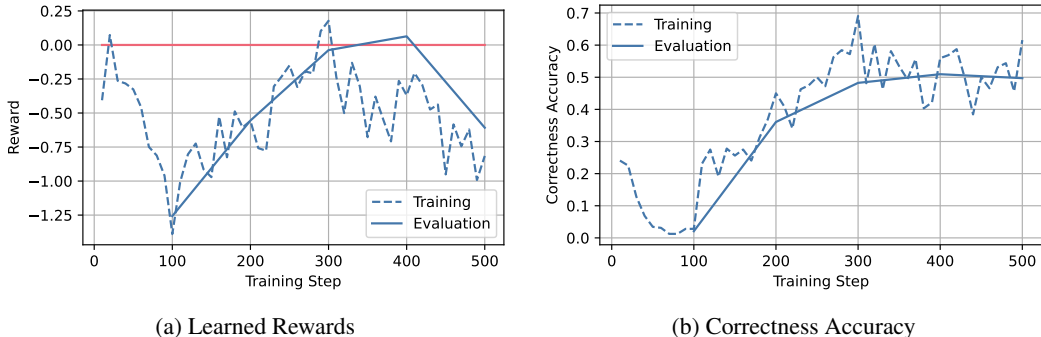


Figure 2: **Training behaviour of the reward and correctness** for Llama3.1-8B as the policy with Llama3.2-1B as the discriminator. Left (2a): aggregate learned reward over training steps (train/eval). Right (2b): correctness accuracy (train/eval).

For completeness, we benchmark predictive performance against two strong references in Appendix C.1: supervised fine-tuning on reasoning traces and GRPO (DeepSeek-AI et al., 2025), which uses verifiable outcome rewards and therefore serves as an empirical upper bound. Appendix Table 2 shows that our expert reasoning approach is frequently competitive with, and sometimes exceeds, supervised fine tuning across $k \in \{1, 3, 5, 10\}$, while GRPO traces the strongest curve. Closing the remaining gap to supervised fine tuning and GRPO in raw pass@1, without sacrificing the dual use of the learned reasoning reward model for training and inference, is promising future work.

Takeaway: The learned dense reward functions are a faithful training signal. Increases in the reward align with improvements in evaluation correctness. Although raw pass@1 can trail strong supervised fine tuning baselines and GRPO, the reasoning reward model’s dual role enables capability gains that the following sections develop.

5.2 INFERENCE TIME ASSISTANCE VIA REWARD-GUIDED RERANKING

We next test whether the learned reward can be used at inference to select better candidates from a small sample budget (Sun and van der Schaar, 2025). For each prompt we draw N candidate traces from the policy, score each trace by the mean discounted token level reward, and pick the top k traces by this score. We report $\text{pass}@k \mid N$, defined as the fraction of prompts for which at least one of the selected k traces is correct when N samples were available in total. Random ranking provides a natural baseline that does not use the reward. Unless stated otherwise we use $N = 16$.

Figure 3 shows results for Llama3.1-B with a Llama3.2-1B discriminator. The left panel displays the distribution of mean discounted rewards for answer tokens, split by whether the final answer is correct or not. The distributions are clearly separated with a large t statistic, and the right panel shows that reward guided reranking improves $\text{pass}@k \mid N$ over random ranking across the range of k . These results indicate that the reward model is calibrated to correctness and that its scores are useful for selection at inference.

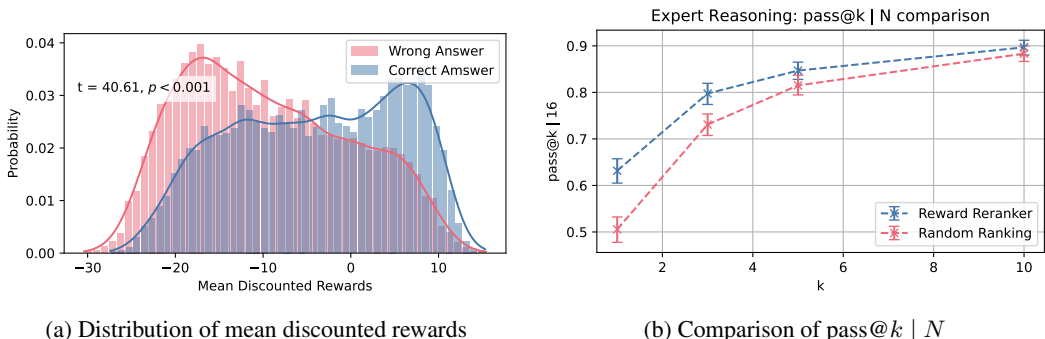


Figure 3: **Benefit of the reasoning reward at inference** for Llama3.1-8B with a Llama3.2-1B critic. Left(3a): reward distributions for correct versus incorrect answers. Right (3b): $\text{pass}@k \mid 16$ using reward-guided reranking versus random ranking.

Appendix B.2 reports the same analysis for Qwen2.5-3B and 7B and Llama3.2-3B in Figures 10, 11, and 12. For Llama3.2-3B, we again observe a clear separation of the reward distributions and consistent gains in $\text{pass}@k \mid 16$. For the Qwen models, reward-guided reranking does not yield statistically significant improvements. Two factors likely explain this outcome. First, the class conditional reward distributions overlap more for Qwen, which weakens the ranking signal. Second, the Qwen2.5 policies are already strong predictors (Table 2 shows Qwen2.5-7B exceeding SFT at $\text{pass}@1$), leaving limited headroom for selection to change the top k . Consequently, the marginal value of reranking is potentially reduced, even when the distributional separation is statistically non-zero.

Takeaway: The learned reward is effective for inference time selection under a fixed budget, with clear $\text{pass}@k \mid N$ gains for Llama3-based policies. For Qwen2.5, despite a statistically significant separation of reward distributions, reranking does not produce significant gains, likely due to the strong base accuracy and weaker separation.

5.3 REWARD PREFERS LIKELY CORRECT TRACES OVER STYLISTIC CONFORMITY

In this experiment, we investigate whether the learned reward is based on correctness rather than superficial formatting. For each response, we compute the mean (discounted) reward over answer tokens and compare it to verifiable signals used in GRPO: a binary correctness indicator and a formatting or structure signal. We report Pearson correlations.

Figure 4 shows the correlation matrix for the Llama3.1-8B policy with Llama3.2-1B discriminator. The learned (discounted) rewards exhibit their strongest association with correctness ($\rho = 0.27$ for rewards, and $\rho = 0.30$ for discounted rewards, $\gamma = 0.9$). At the same time, correlations with formatting-based signals (XML Count, Strict Format, Soft Format, and integer response) are appreciably smaller. This pattern indicates that the reasoning reward model scores are calibrated to solution validity rather than to the presence of a particular structure, which is consistent with the separation observed in the reward distributions and with the improvements from reranking in subsection 5.2. Additional correlation matrices for other backbones are reported in Appendix B.3 in Figure 13.

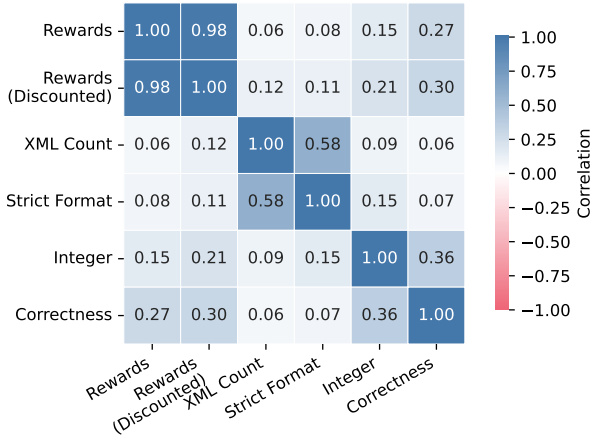


Figure 4: **Correlation of the learned reward** for Llama3.1-8B with Llama3.2-1B. Shows correlations between the (discounted) learned reward on answer tokens and verifiable signals: correctness and formatting structure.

To improve robustness, we introduce perturbed samples during training for both expert and policy traces. The perturbations flip operator signs, corrupt numbers, and swap the final answer with a previous intermediate number. The perturbations expose near-miss errors that share surface form with correct traces but are semantically incorrect. In Appendix C.3, we report our experiment comparing training with and without perturbations in Figure 18. With perturbations, the reward distributions for correct and incorrect answers separate more clearly, the $\text{pass}@k \mid N$ curves improve at low k , and the correlations with formatting signals decreases.

Takeaway: The learned reward correlates most strongly with correctness and only weakly with formatting, indicating a preference for likely correct traces rather than stylistic conformity. Training with targeted perturbations further sharpens this preference and improves selection behaviour.

5.4 INTERPRETABLE DENSE REWARDS AND LOCALISATION OF ERRORS

We evaluate whether the learned dense reward provides actionable interpretability by revealing where a reasoning trace succeeds or fails. We visualise token-level normalised rewards along the trace and focus on the answer region with discount factor $\gamma = 0.9$. Here, we display one correct and one incorrect example for Llama3.1-8B with a Llama3.2-1B discriminator (Figures 5 and 6); the appendix provides two additional correct and two additional incorrect examples per backbone for both Llama3 and Qwen2.5 combination (Appendix B.4, Figures 14, 15, and 16).

In correct solutions the reward forms contiguous positive bands that align with decisive computations and algebraic simplifications, with neutral or slightly positive rewards on connective tokens. In incorrect solutions we observe early negative bands at the point of deviation, followed by persistently negative or oscillating rewards. The penalties propagate forward due to discounting, which makes the final answer region strongly negative even when surface level formatting remains plausible. These patterns are consistent across backbones and mirror the distributional separation and reranking gains reported in subsections 5.1 and 5.2.

Takeaway: The learned dense reward yields interpretable token-level attributions that pinpoint failure and reveal error propagation, enabling auditing and simple triggers for early rejection or self-revision. A natural extension and interesting option for future work is reward-guided next-token generation to self-correct when a trace begins to drift.

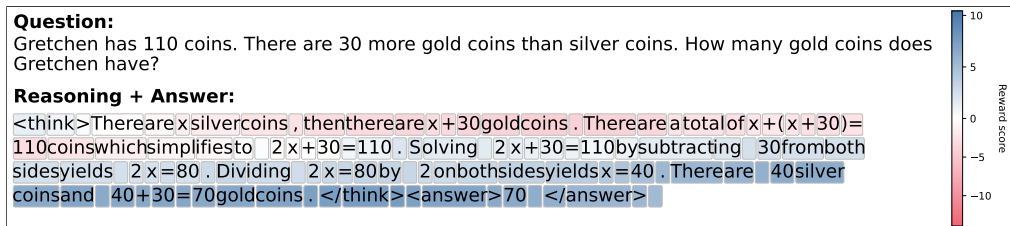


Figure 5: **Correct answering.** Dense reward on a correct solution shows contiguous positive bands on decisive computations. Rewards are standardised and discounted with $\gamma = 0.9$.

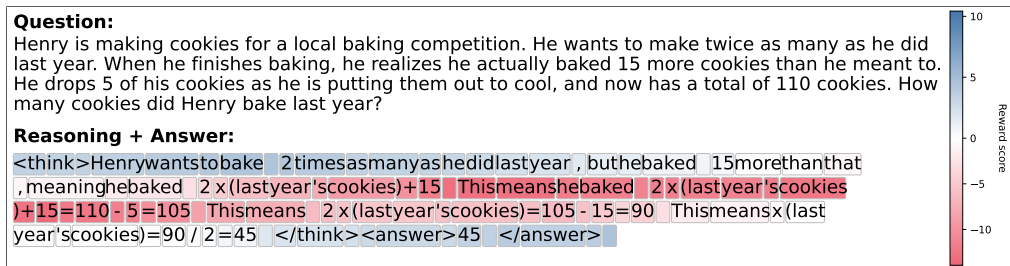


Figure 6: **Incorrect answering.** Dense reward on an incorrect solution highlights the first erroneous step with a sharp negative band, followed by propagated penalties into later tokens and the final answer due to discounting. Rewards are standardised and discounted with $\gamma = 0.9$.

6 LIMITATIONS

Our approach has several limitations. Joint optimisation of the policy and learned reward can lag SFT in pass@1 on some backbones. The discriminator may inherit bias or noise from expert traces, and adversarial training yields non-stationary signals. Learned rewards can overfit to superficial cues, and calibration differs across model families, with weaker separation for Qwen2.5 compared to Llama3. Performance depends on choices such as discounting, token aggregation, and normalisation. Compute and latency rise due to alternating updates and inference-time scoring. Finally, evaluation is limited to GSM8K-style arithmetic reasoning and does not cover long context, multimodality, or high-stakes settings.

7 FUTURE WORK

A learned dense reward can serve as both a training signal and an inference-time assistant, providing token-level diagnostics. Several directions follow. First, close the remaining pass@1 gap to strong SFT by improving optimisation at the discriminator-policy interface; to this end we also explored a Wasserstein GAN (Arjovsky et al., 2017) variant (Appendix C.4). Second, improve reward calibration across backbones, especially Qwen2.5, via refined perturbations, hard negatives, and contrastive objectives. Third, integrate the critic at generation time through reward-guided decoding, early rejection, and self-revision. Fourth, extend beyond GSM8K to broader domains and to settings with limited or noisy demonstrations, including online learning and active data collection.

8 CONCLUSION

We introduced an inverse reinforcement learning approach that learns a dense reasoning reward from expert demonstrations. The learned critic serves two roles. It teaches a policy to reason through token-level feedback, and it improves predictive performance at inference by reranking under a fixed sampling budget. The reward aligns with correctness rather than surface form and offers interpretable localisation of errors. While raw accuracy may trail strong supervised fine-tuning and outcome-reward RL, the capability gains are clear. We view this work as a step toward reusable process-level critics that support training, inference, and diagnosis in a single framework.

ACKNOWLEDGEMENTS AND DISCLOSURE OF FUNDING

We want to extend our gratitude to Kasia Kobalczyk, Paulius Rauba, Yusuke Kano, Jeremy Voisey, and Alison O’Neil for their insightful discussions and valuable feedback. Canon Medical Systems Corporation funds CF’s studentship. The W.D. Armstrong Trust Fund and the Cystic Fibrosis Fund support NA’s studentship. This work was supported by Microsoft’s Accelerate Foundation Models Academic Research initiative.

REFERENCES

- DeepSeek-AI, Daya Guo, Dejian Yang, Haowei Zhang, Junxiao Song, Ruoyu Zhang, Runxin Xu, Qihao Zhu, Shirong Ma, Peiyi Wang, Xiao Bi, Xiaokang Zhang, Xingkai Yu, Yu Wu, Z. F. Wu, Zhibin Gou, Zhihong Shao, Zhuoshu Li, Ziyi Gao, Aixin Liu, Bing Xue, Bingxuan Wang, Bochao Wu, Bei Feng, Chengda Lu, Chenggang Zhao, Chengqi Deng, Chenyu Zhang, Chong Ruan, Damai Dai, Deli Chen, Dongjie Ji, Erhang Li, Fangyun Lin, Fucong Dai, Fuli Luo, Guangbo Hao, Guanting Chen, Guowei Li, H. Zhang, Han Bao, Hanwei Xu, Haocheng Wang, Honghui Ding, Huajian Xin, Huazuo Gao, Hui Qu, Hui Li, Jianzhong Guo, Jiashi Li, Jiawei Wang, Jingchang Chen, Jingyang Yuan, Junjie Qiu, Junlong Li, J. L. Cai, Jiaqi Ni, Jian Liang, Jin Chen, Kai Dong, Kai Hu, Kaige Gao, Kang Guan, Kexin Huang, Kuai Yu, Lean Wang, Lecong Zhang, Liang Zhao, Litong Wang, Liyue Zhang, Lei Xu, Leyi Xia, Mingchuan Zhang, Minghua Zhang, Minghui Tang, Meng Li, Miaojun Wang, Mingming Li, Ning Tian, Panpan Huang, Peng Zhang, Qiancheng Wang, Qinyu Chen, Qiushi Du, Ruiqi Ge, Ruisong Zhang, Ruizhe Pan, Runji Wang, R. J. Chen, R. L. Jin, Ruyi Chen, Shanghao Lu, Shangyan Zhou, Shanhuang Chen, Shengfeng Ye, Shiyu Wang, Shuiping Yu, Shunfeng Zhou, Shuting Pan, S. S. Li, Shuang Zhou, Shaoqing Wu, Shengfeng Ye, Tao Yun, Tian Pei, Tianyu Sun, T. Wang, Wangding Zeng, Wanbiao Zhao, Wen Liu, Wenfeng Liang, Wenjun Gao, Wenqin Yu, Wentao Zhang, W. L. Xiao, Wei An, Xiaodong Liu, Xiaohan Wang, Xiaokang Chen, Xiaotao Nie, Xin Cheng, Xin Liu, Xin Xie, Xingchao Liu, Xinyu Yang, Xinyuan Li, Xuecheng Su, Xuheng Lin, X. Q. Li, Xiangyue Jin, Xiaojin Shen, Xiaosha Chen, Xiaowen Sun, Xiaoxiang Wang, Xinnan Song, Xinyi Zhou, Xianzu Wang, Xinxia Shan, Y. K. Li, Y. Q. Wang, Y. X. Wei, Yang Zhang, Yanhong Xu, Yao Li, Yao Zhao, Yaofeng Sun, Yaohui Wang, Yi Yu, Yichao Zhang, Yifan Shi, Yiliang Xiong, Ying He, Yishi Piao, Yisong Wang, Yixuan Tan, Yiyang Ma, Yiyuan Liu, Yongqiang Guo, Yuan Ou, Yuduan Wang, Yue Gong, Yuheng Zou, Yujia He, Yunfan Xiong, Yuxiang Luo, Yuxiang You, Yuxuan Liu, Yuyang Zhou, Y. X. Zhu, Yanhong Xu, Yanping Huang, Yaohui Li, Yi Zheng, Yuchen Zhu, Yunxian Ma, Ying Tang, Yukun Zha, Yuting Yan, Z. Z. Ren, Zehui Ren, Zhangli Sha, Zhe Fu, Zhean Xu, Zhenda Xie, Zhengyan Zhang, Zhewen Hao, Zhicheng Ma, Zhigang Yan, Zhiyu Wu, Zihui Gu, Zijia Zhu, Zijun Liu, Zilin Li, Ziwei Xie, Ziyang Song, Zizheng Pan, Zhen Huang, Zhipeng Xu, Zhongyu Zhang, and Zhen Zhang. DeepSeek-R1: Incentivizing Reasoning Capability in LLMs via Reinforcement Learning, January 2025. URL <http://arxiv.org/abs/2501.12948>. arXiv:2501.12948 [cs].
- Amrith Setlur, Nived Rajaraman, Sergey Levine, and Aviral Kumar. Scaling Test-Time Compute Without Verification or RL is Suboptimal, February 2025. URL <http://arxiv.org/abs/2502.12118>. arXiv:2502.12118 [cs].
- Hao Sun and Mihaela van der Schaar. Inverse-RLignment: Large Language Model Alignment from Demonstrations through Inverse Reinforcement Learning, January 2025. URL <http://arxiv.org/abs/2405.15624>. arXiv:2405.15624 [cs].
- Jonathan Uesato, Nate Kushman, Ramana Kumar, Francis Song, Noah Siegel, Lisa Wang, Antonia Creswell, Geoffrey Irving, and Irina Higgins. Solving math word problems with process- and outcome-based feedback, November 2022. URL <http://arxiv.org/abs/2211.14275>. arXiv:2211.14275 [cs].
- Hunter Lightman, Vineet Kosaraju, Yura Burda, Harri Edwards, Bowen Baker, Teddy Lee, Jan Leike, John Schulman, Ilya Sutskever, and Karl Cobbe. Let’s Verify Step by Step, May 2023. URL <http://arxiv.org/abs/2305.20050>. arXiv:2305.20050 [cs].
- Eric Zelikman, Yuhuai Wu, Jesse Mu, and Noah D. Goodman. STaR: Bootstrapping Reasoning With Reasoning, May 2022. URL <http://arxiv.org/abs/2203.14465>. arXiv:2203.14465 [cs].

- Zheng Yuan, Hongyi Yuan, Chengpeng Li, Guanting Dong, Keming Lu, Chuanqi Tan, Chang Zhou, and Jingren Zhou. Scaling Relationship on Learning Mathematical Reasoning with Large Language Models, September 2023. URL <http://arxiv.org/abs/2308.01825>. arXiv:2308.01825 [cs].
- Avi Singh, John D. Co-Reyes, Rishabh Agarwal, Ankesh Anand, Piyush Patil, Xavier Garcia, Peter J. Liu, James Harrison, Jaehoon Lee, Kelvin Xu, Aaron T. Parisi, Abhishek Kumar, Alexander A. Alemi, Alex Rizkowsky, Azade Nova, Ben Adlam, Bernd Bohnet, Gamaleldin Fathy Elsayed, Hanie Sedghi, Igor Mordatch, Isabelle Simpson, Izzeddin Gur, Jasper Snoek, Jeffrey Pennington, Jiri Hron, Kathleen Kenealy, Kevin Swersky, Kshiteej Mahajan, Laura A. Culp, Lechao Xiao, Maxwell Bileschi, Noah Constant, Roman Novak, Rosanne Liu, Tris Warkentin, Yamini Bansal, Ethan Dyer, Behnam Neyshabur, Jascha Sohl-Dickstein, and Noah Fiedel. Beyond Human Data: Scaling Self-Training for Problem-Solving with Language Models. *Transactions on Machine Learning Research*, January 2024. ISSN 2835-8856. URL <https://openreview.net/forum?id=lNAyUngGFK>.
- Arian Hosseini, Xingdi Yuan, Nikolay Malkin, Aaron Courville, Alessandro Sordoni, and Rishabh Agarwal. V-STaR: Training Verifiers for Self-Taught Reasoners. August 2024. URL <https://openreview.net/forum?id=stmqBSW2dV#discussion>.
- David Silver, Julian Schrittwieser, Karen Simonyan, Ioannis Antonoglou, Aja Huang, Arthur Guez, Thomas Hubert, Lucas baker, Matthew Lai, Adrian Bolton, Yutian Chen, Timothy P. Lillicrap, Fan Hui, L. Sifre, George van den Driessche, Thore Graepel, and Demis Hassabis. Mastering the game of go without human knowledge. *Nature*, 550:354–359, 2017. URL <https://api.semanticscholar.org/CorpusID:205261034>.
- Ganqu Cui, Lifan Yuan, Zefan Wang, Hanbin Wang, Wendi Li, Bingxiang He, Yuchen Fan, Tianyu Yu, Qixin Xu, Weize Chen, Jiarui Yuan, Huayu Chen, Kaiyan Zhang, Xingtai Lv, Shuo Wang, Yuan Yao, Xu Han, Hao Peng, Yu Cheng, Zhiyuan Liu, Maosong Sun, Bowen Zhou, and Ning Ding. Process Reinforcement through Implicit Rewards, February 2025. URL <http://arxiv.org/abs/2502.01456>. arXiv:2502.01456 [cs].
- Rafael Rafailov, Archit Sharma, Eric Mitchell, Stefano Ermon, Christopher D. Manning, and Chelsea Finn. Direct Preference Optimization: Your Language Model is Secretly a Reward Model, July 2024. URL <http://arxiv.org/abs/2305.18290>. arXiv:2305.18290.
- Brian D Ziebart, Andrew Maas, J Andrew Bagnell, and Anind K Dey. Maximum Entropy Inverse Reinforcement Learning. 2004.
- Pieter Abbeel and Andrew Y. Ng. Apprenticeship learning via inverse reinforcement learning. In *Twenty-first international conference on Machine learning - ICML '04*, page 1, Banff, Alberta, Canada, 2004. ACM Press. doi: 10.1145/1015330.1015430. URL <http://portal.acm.org/citation.cfm?doid=1015330.1015430>.
- Joey Hejna and Dorsa Sadigh. Inverse Preference Learning: Preference-based RL without a Reward Function. 2023.
- Justin Fu, Anoop Korattikara, Sergey Levine, and Sergio Guadarrama. FROM LANGUAGE TO GOALS: INVERSE REINFORCEMENT LEARNING FOR VISION-BASED INSTRUCTION FOLLOWING. 2019.
- Jonathan Ho and Stefano Ermon. Generative Adversarial Imitation Learning, June 2016. URL <http://arxiv.org/abs/1606.03476>. arXiv:1606.03476 [cs].
- Paul Christiano, Jan Leike, Tom B. Brown, Miljan Martic, Shane Legg, and Dario Amodei. Deep reinforcement learning from human preferences, February 2023. URL <http://arxiv.org/abs/1706.03741>. arXiv:1706.03741.
- Hao Sun and Mihaela van der Schaar. Inverse-RLignment: Inverse Reinforcement Learning from Demonstrations for LLM Alignment, May 2024. URL <http://arxiv.org/abs/2405.15624>. arXiv:2405.15624 [cs].

- Han Xia, Songyang Gao, Qiming Ge, Zhiheng Xi, Qi Zhang, and Xuanjing Huang. Inverse-Q*: Token Level Reinforcement Learning for Aligning Large Language Models Without Preference Data, August 2024. URL <http://arxiv.org/abs/2408.14874>. arXiv:2408.14874 [cs].
- Hao Sun and Mihaela van der Schaar. Inverse Reinforcement Learning Meets Large Language Model Post-Training: Basics, Advances, and Opportunities, July 2025. URL <http://arxiv.org/abs/2507.13158>. arXiv:2507.13158 [cs].
- Jared Joselowitz, Arjun Jagota, Satyapriya Krishna, and Sonali Parbhoo. Insights from the Inverse: Reconstructing LLM Training Goals Through Inverse RL, October 2024. URL <http://arxiv.org/abs/2410.12491>. arXiv:2410.12491 [cs].
- Justin Fu, Katie Luo, and Sergey Levine. Learning Robust Rewards with Adversarial Inverse Reinforcement Learning, August 2018. URL <http://arxiv.org/abs/1710.11248>. arXiv:1710.11248 [cs].
- Jiahao Lin and Zongzhang Zhang. ACGAIL: Imitation Learning About Multiple Intentions with Auxiliary Classifier GANs. In Xin Geng and Byeong-Ho Kang, editors, *PRICAI 2018: Trends in Artificial Intelligence*, pages 321–334, Cham, 2018. Springer International Publishing. ISBN 978-3-319-97304-3. doi: 10.1007/978-3-319-97304-3_25.
- Yunzhu Li, Jiaming Song, and Stefano Ermon. InfoGAIL: Interpretable Imitation Learning from Visual Demonstrations, November 2017. URL <http://arxiv.org/abs/1703.08840>. arXiv:1703.08840 [cs].
- Geoffrey Hinton, Oriol Vinyals, and Jeff Dean. Distilling the Knowledge in a Neural Network, March 2015. URL <http://arxiv.org/abs/1503.02531>. arXiv:1503.02531 [stat].
- Minki Kang, Seanie Lee, Jinheon Baek, Kenji Kawaguchi, and Sung Ju Hwang. Knowledge-Augmented Reasoning Distillation for Small Language Models in Knowledge-Intensive Tasks. In A. Oh, T. Naumann, A. Globerson, K. Saenko, M. Hardt, and S. Levine, editors, *Advances in Neural Information Processing Systems*, volume 36, pages 48573–48602. Curran Associates, Inc., 2023. URL https://proceedings.neurips.cc/paper_files/paper/2023/file/97faedc90260eae5c400f92d5831c3d7-Paper-Conference.pdf.
- Kalle Kujanpää, Pekka Marttinen, Harri Valpola, and Alexander Ilin. Efficient Knowledge Injection in LLMs via Self-Distillation, August 2025. URL <http://arxiv.org/abs/2412.14964>. arXiv:2412.14964 [cs].
- Hongling Xu, Qi Zhu, Heyuan Deng, Jinpeng Li, Lu Hou, Yasheng Wang, Lifeng Shang, Ruifeng Xu, and Fei Mi. KDRL: Post-Training Reasoning LLMs via Unified Knowledge Distillation and Reinforcement Learning, June 2025. URL <http://arxiv.org/abs/2506.02208>. arXiv:2506.02208 [cs].
- Ian J. Goodfellow, Jean Pouget-Abadie, Mehdi Mirza, Bing Xu, David Warde-Farley, Sherjil Ozair, Aaron Courville, and Yoshua Bengio. Generative Adversarial Networks, June 2014. URL <http://arxiv.org/abs/1406.2661>. arXiv:1406.2661 [stat].
- Siyao Zhao, John Dang, and Aditya Grover. Group Preference Optimization: Few-Shot Alignment of Large Language Models, October 2024. URL <http://arxiv.org/abs/2310.11523>. arXiv:2310.11523.
- John Schulman, Filip Wolski, Prafulla Dhariwal, Alec Radford, and Oleg Klimov. Proximal Policy Optimization Algorithms, August 2017. URL <http://arxiv.org/abs/1707.06347>. arXiv:1707.06347 [cs].
- Karl Cobbe, Vineet Kosaraju, Mohammad Bavarian, Mark Chen, Heewoo Jun, Lukasz Kaiser, Matthias Plappert, Jerry Tworek, Jacob Hilton, Reiichiro Nakano, Christopher Hesse, and John Schulman. Training Verifiers to Solve Math Word Problems, November 2021. URL <http://arxiv.org/abs/2110.14168>. arXiv:2110.14168 [cs].

Jinze Bai, Shuai Bai, Yunfei Chu, Zeyu Cui, Kai Dang, Xiaodong Deng, Yang Fan, Wenbin Ge, Yu Han, Fei Huang, Binyuan Hui, Luo Ji, Mei Li, Junyang Lin, Runji Lin, Dayiheng Liu, Gao Liu, Chengqiang Lu, Keming Lu, Jianxin Ma, Rui Men, Xingzhang Ren, Xuancheng Ren, Chuanqi Tan, Sinan Tan, Jianhong Tu, Peng Wang, Shijie Wang, Wei Wang, Shengguang Wu, Benfeng Xu, Jin Xu, An Yang, Hao Yang, Jian Yang, Shusheng Yang, Yang Yao, Bowen Yu, Hongyi Yuan, Zheng Yuan, Jianwei Zhang, Xingxuan Zhang, Yichang Zhang, Zhenru Zhang, Chang Zhou, Jingren Zhou, Xiaohuan Zhou, and Tianhang Zhu. Qwen Technical Report, September 2023. URL <http://arxiv.org/abs/2309.16609>. arXiv:2309.16609 [cs].

Hugo Touvron, Thibaut Lavril, Gautier Izacard, Xavier Martinet, Marie-Anne Lachaux, Timothée Lacroix, Baptiste Rozière, Naman Goyal, Eric Hambro, Faisal Azhar, Aurelien Rodriguez, Armand Joulin, Edouard Grave, and Guillaume Lample. LLaMA: Open and Efficient Foundation Language Models, February 2023. URL <http://arxiv.org/abs/2302.13971>. arXiv:2302.13971 [cs].

Martin Arjovsky, Soumith Chintala, and Léon Bottou. Wasserstein GAN, December 2017. URL <http://arxiv.org/abs/1701.07875>. arXiv:1701.07875 [stat].

Guido Van Rossum and Fred L Drake Jr. *Python reference manual*. Centrum voor Wiskunde en Informatica Amsterdam, 1995.

Adam Paszke, Sam Gross, Soumith Chintala, Gregory Chanan, Edward Yang, Zachary DeVito, Zeming Lin, Alban Desmaison, Luca Antiga, and Adam Lerer. Automatic differentiation in pytorch. 2017.

Thomas Wolf, Lysandre Debut, Victor Sanh, Julien Chaumond, Clement Delangue, Anthony Moi, Pierric Cistac, Tim Rault, Rémi Louf, Morgan Funtowicz, Joe Davison, Sam Shleifer, Patrick von Platen, Clara Ma, Yacine Jernite, Julien Plu, Canwen Xu, Teven Le Scao, Sylvain Gugger, Mariama Drame, Quentin Lhoest, and Alexander M. Rush. HuggingFace’s Transformers: State-of-the-art Natural Language Processing, July 2020. URL <http://arxiv.org/abs/1910.03771>. arXiv:1910.03771 [cs].

Michael Han Daniel Han and Unsloth team. Unsloth, 2023. URL <http://github.com/unslothai/unsloth>.

A IMPLEMENTATION DETAILS

We evaluate the proposed expert reasoning approach on GSM8K, a benchmark of grade school mathematics problems that provides final answers and human-written demonstrations. Unless noted otherwise, we use open-weight instruction-tuned models as base policies and train a learned reward using adversarial inverse reinforcement learning. When the reward model is implemented as a sequence classifier, it yields a sparse signal at the sequence level. To obtain a dense signal, we instead implement the discriminator as a token classifier that shares the backbone with a language model and replaces the language modelling head with a single linear layer that outputs one logit per token. The code to all our experiments can be found at https://github.com/fanconic/expert_reasoning.

All experiments are implemented in Python (Van Rossum and Drake Jr, 1995) with PyTorch (Paszke et al., 2017) and Hugging Face Transformers (Wolf et al., 2020). We accelerate training and evaluation with UNSLOTH (Daniel Han and team, 2023). Unless stated otherwise we use a starting learning rate of 1×10^{-5} for both policy and discriminator (1×10^{-4} for the Llama models) with a cosine schedule and ten per cent warm up. We train for 500 optimisation steps with batch size 16 and generate $G = 16$ samples per prompt, accumulated over two gradient steps.

Data and preprocessing. We follow the standard GSM8K split. Prompts consist of the problem text with a short system instruction that requests step by step reasoning. Demonstrations are formatted as `<think> ... </think>` followed by `<answer> ... </answer>` format. Tokenisation uses the native tokeniser of each backbone. For evaluation, we decode with temperature $T = 1.0$ and $\text{top}_p = 0.95$ unless stated otherwise.

Objectives and optimisation. The discriminator is trained with a binary cross entropy objective to distinguish expert traces from policy traces at the token level. Let $r_\phi(y_t | x, y_{<t})$ denote the reward at token t ; the aggregate trace reward is the mean of discounted rewards over the answer segment with discount factor $\gamma = 0.9$. Policy updates follow a group wise normalised advantage objective with G samples per prompt. We apply gradient clipping, weight decay ($\beta_1 = 0.9, \beta_2 = 0.99$), and label smoothing (0.95) on the discriminator targets. We use a quantised ADAM optimiser.

Inference time scoring. At inference we draw $N = 16$ samples per prompt, compute the mean discounted reward over answer tokens for each sample, and rerank by this score. We report $\text{pass}@k | N$, the fraction of prompts for which at least one of the top k ranked samples is correct when N samples are available. Unless noted otherwise $N = 16$ and $k \in \{1, 3, 5, 10\}$.

Perturbations. To improve robustness and reduce reliance on surface form we introduce targeted perturbations during discriminator training for both expert and policy traces: (i) flip arithmetic operator signs, (ii) corrupt numeric literals by small random offsets, and (iii) swap the final answer with an earlier intermediate number. Perturbed traces are labelled as non expert.

Compute. Experiments are conducted on A100-class GPUs with mixed-precision training. We use gradient accumulation to match effective batch sizes across backbones. All models are in 4-bit mode, provided by UNSLOTH (Daniel Han and team, 2023) for training speed and memory efficiency.

A.1 POLICY MODEL

Policies are initialised from instruction-tuned checkpoints and trained with the learned reward signal. The following policy backbones are used:

- Llama3.1-8B-Instruct
- Llama3.2-3B-Instruct
- Qwen 2.5-3B-Instruct
- Qwen 2.5-7B-Instruct

A.2 DISCRIMINATOR MODEL

Unless specified otherwise the discriminator shares the architecture family with the policy but differs in size. The discriminator is always trained as a token classifier:

- Llama3.2-1B-Instruct
- Qwen-2.5-0.5B-Instruct
- Qwen-2.5-1.5B-Instruct
- Qwen-2.5-Math-1.5B-Instruct (*ablation*)

A.3 POLICY-DISCRIMINATOR COMBINATIONS

We evaluate the following pairings; results for the representative configuration appear in the main text, and the remainder in the appendix:

Policy	Discriminator
Llama3.1-8B-Instruct	Llama3.2-1B-Instruct
Llama3.2-3B-Instruct	Llama3.2-3B-Instruct
Qwen-2.5-3B-Instruct	Qwen-2.5-0.5B-Instruct
Qwen-2.5-7B-Instruct	Qwen-2.5-1.5B-Instruct
Qwen-2.5-7B-Instruct	Qwen-2.5-0.5B-Instruct (<i>ablation</i>)
Qwen-2.5-7B-Instruct	Qwen-2.5-Math-1.5B-Instruct (<i>ablation</i>)

For completeness, we also test a maths-specialised variant of the discriminator within the Qwen family; it does not improve calibration relative to the general-purpose discriminator in our setting and is therefore reported only in the Appendix C.2.

A.4 STATEMENT ABOUT THE USE OF LARGE LANGUAGE MODELS

We utilised large language models to assist with drafting and editing the manuscript, as well as to accelerate implementation by generating boilerplate code and providing debugging suggestions. LLMs were not involved in the conception of the methods, study design, or interpretation of results. All outputs were reviewed and verified by the authors, who take full responsibility for the content.

B ADDITIONAL RESULTS

B.1 TRAINING BEHAVIOUR

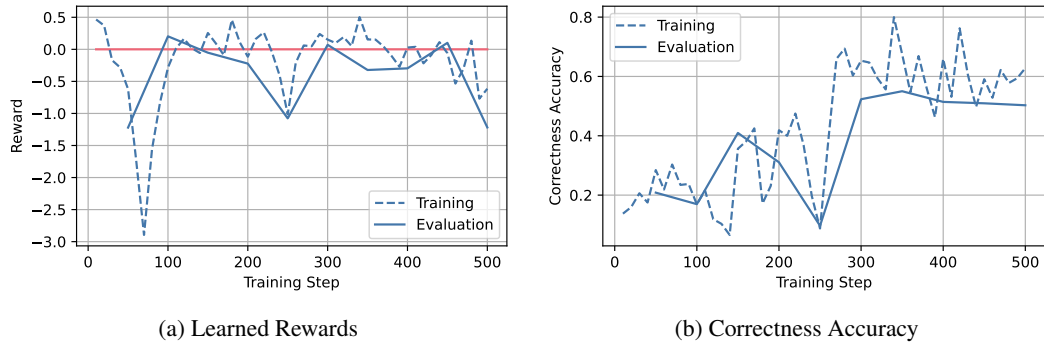


Figure 7: **Training behaviour of the Reward and Correctness.** Subfigure 7a shows the training and evaluation reward during optimisation, and Subfigure 7b demonstrates the increasing correctness for the (Qwen2.5-3B-Instruct - Qwen2.5-0.5B-Instruct) combination.

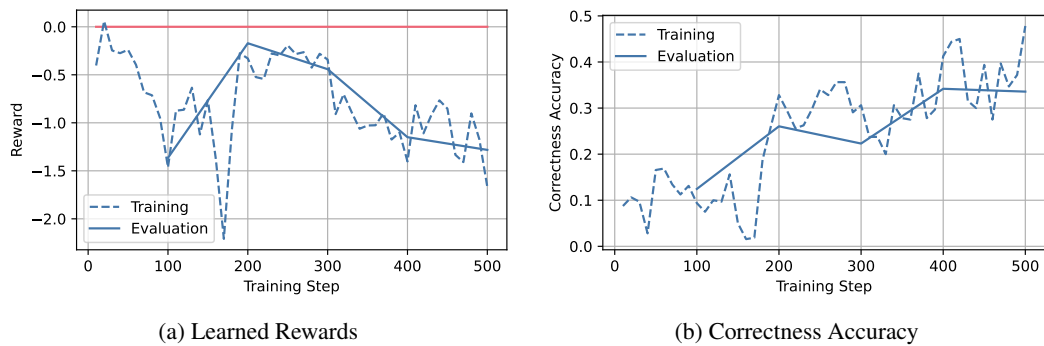


Figure 8: **Training behaviour of the Reward and Correctness.** Subfigure 8a shows the training and evaluation reward during optimisation, and Subfigure 8b demonstrates the increasing correctness for the (Llama3.1-3B-Instruct - Llama3.2-1B-Instruct) combination.

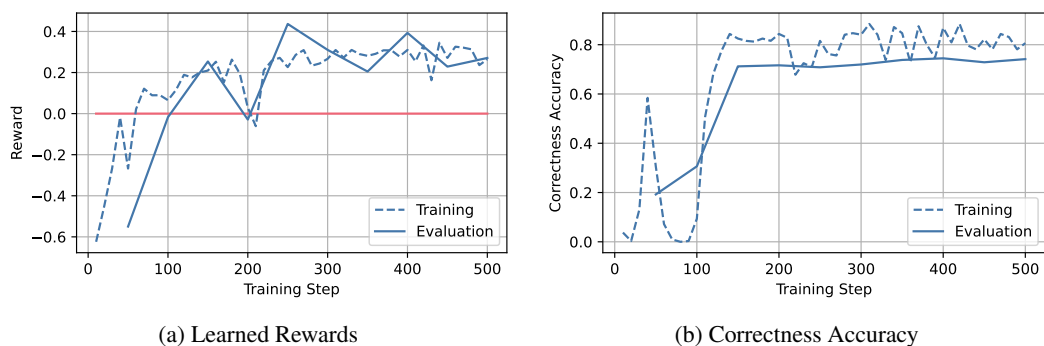


Figure 9: **Training behaviour of the Reward and Correctness.** Subfigure 9a shows the training and evaluation reward during optimisation, and Subfigure 9b demonstrates the increasing correctness for the (Qwen2.5-7B-Instruct - Qwen2.5-1.5B-Instruct) combination.

B.2 DISTRIBUTION OF REWARDS AND RERANKING PERFORMANCE

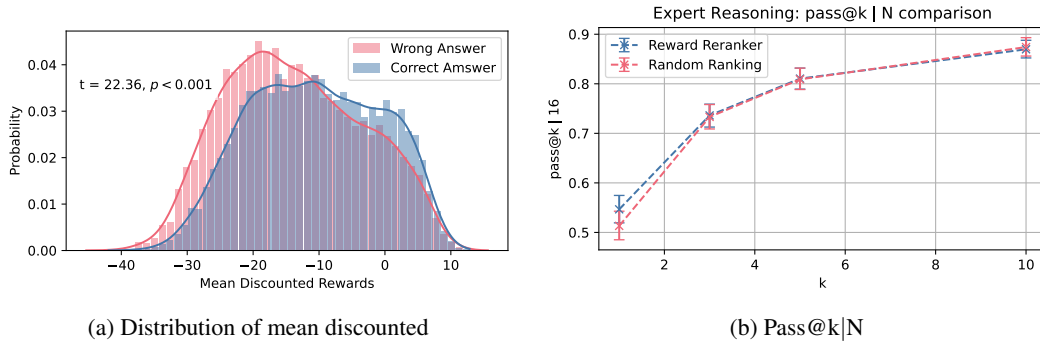


Figure 10: **Benefit of Reasoning Reward Model.** This is for the (Qwen2.5-3B-Instruct - Qwen2.5-0.5B-Instruct) combination.

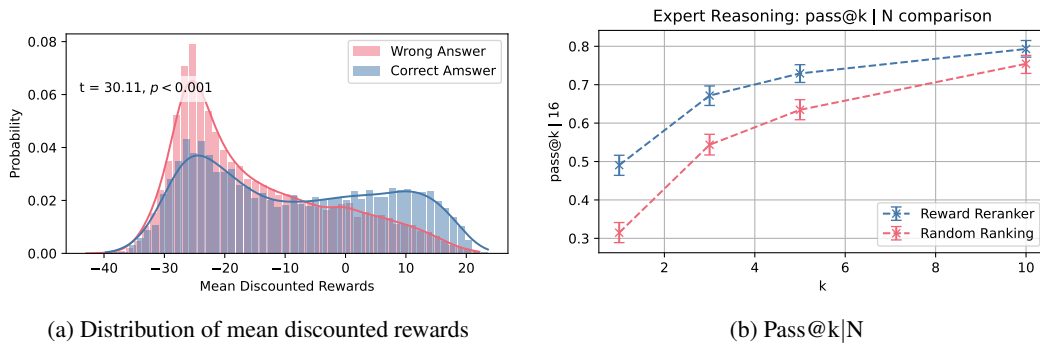


Figure 11: **Benefit of Reasoning Reward Model.** This is for the (Llama3.2-3B-Instruct - Llama3.2-1B-Instruct) combination.

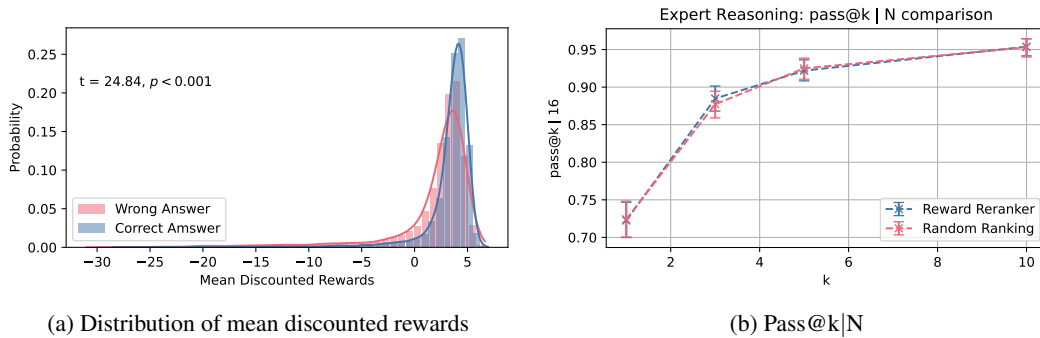


Figure 12: **Benefit of Reasoning Reward Model.** This is for the (Qwen2.5-7B-Instruct - Qwen2.5-1.5B-Instruct) combination.

B.3 CORRELATION OF REWARD MODEL WITH CORRECTNESS AND FORMATTING

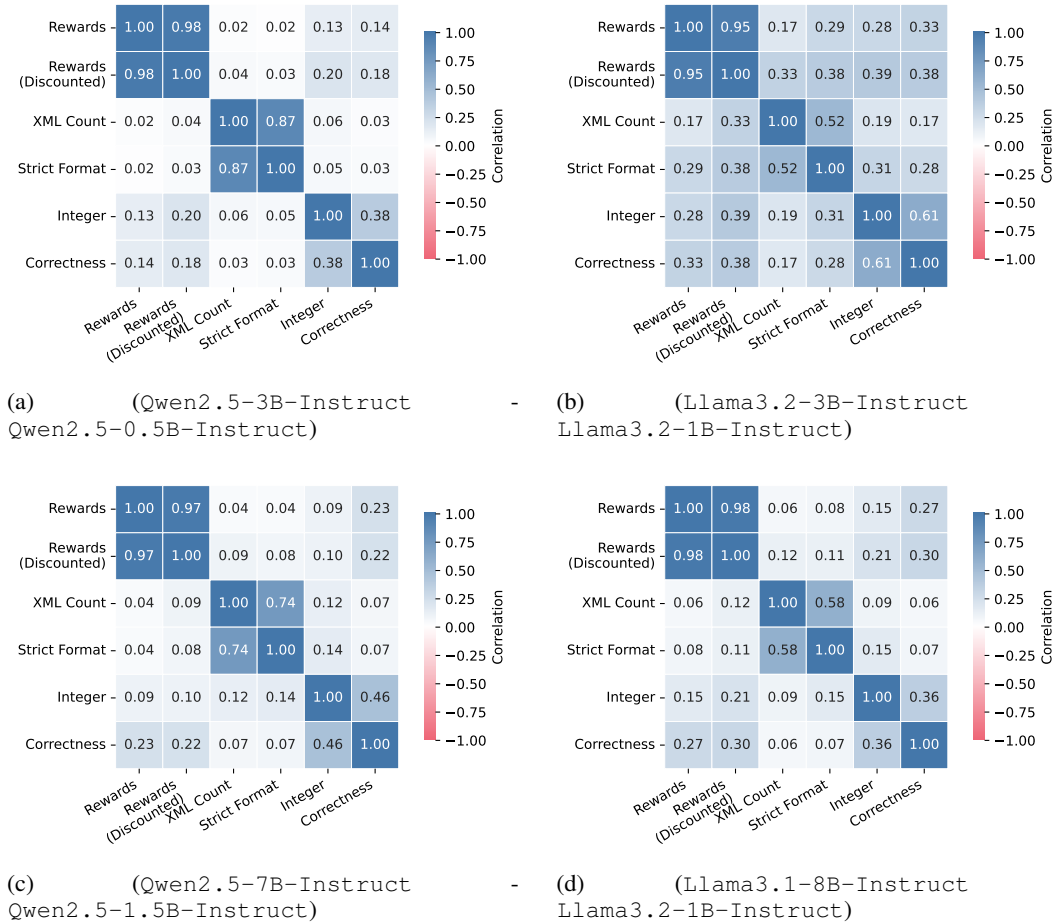
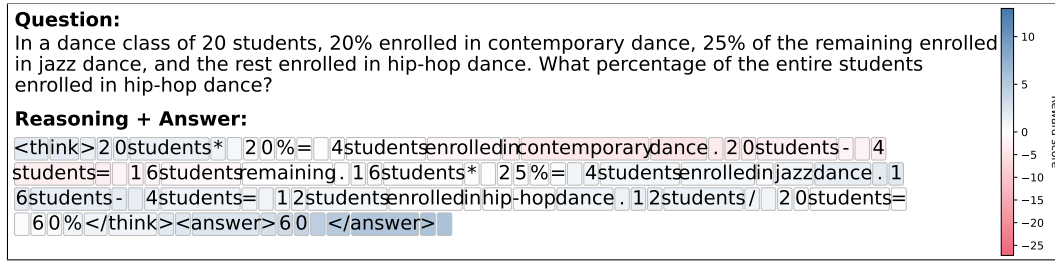
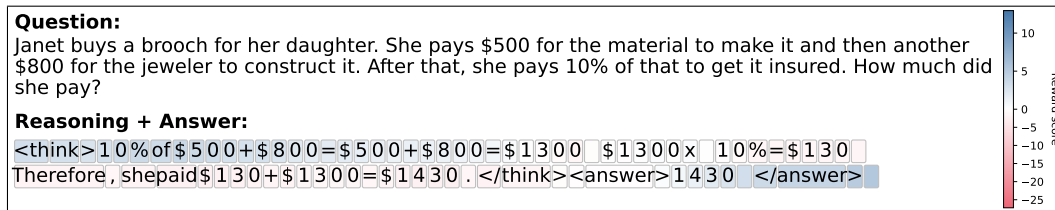


Figure 13: **Correlation Matrix of Verifiable Rewards with Learned Reward.** Correlation between the mean rewards of the answer tokens with the various verifiable rewards, used in GRPO training. We are especially interested in the correlation between correctness and the rewards.

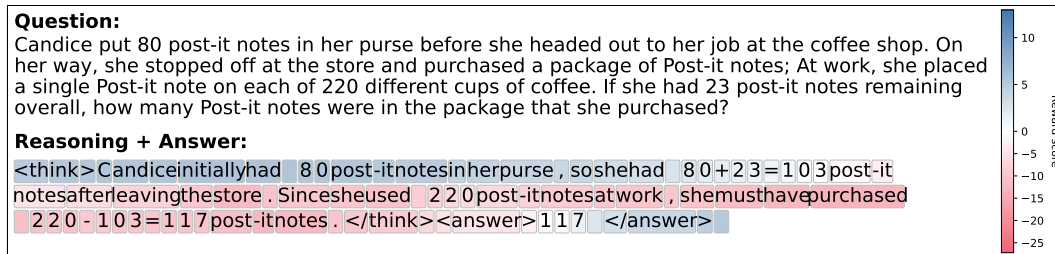
B.4 REASONING TRACES



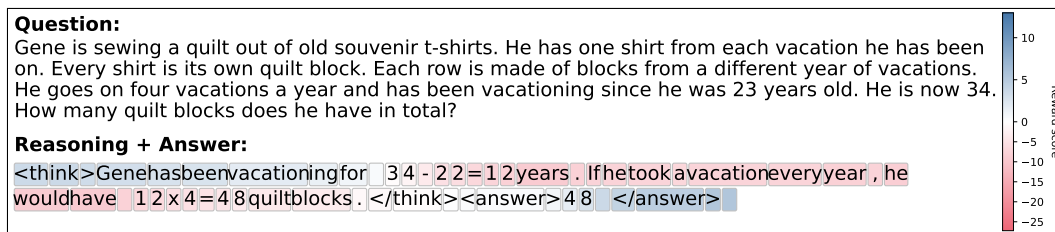
(a) Correct example 1



(b) Correct example 2

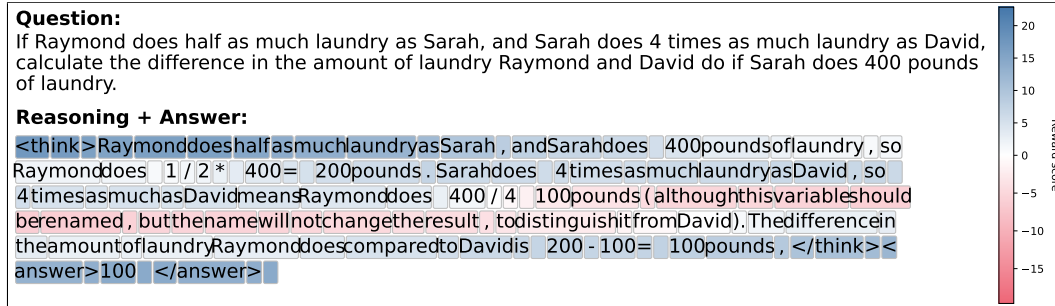


(c) Wrong example 1

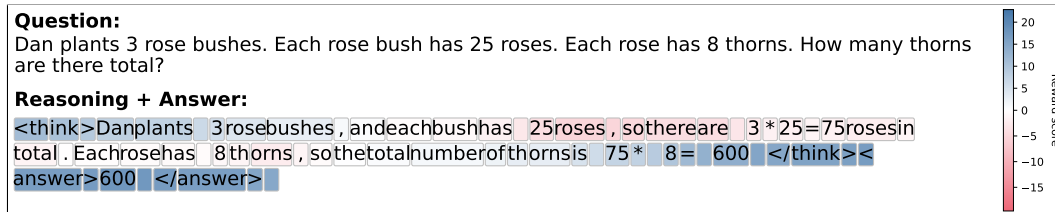


(d) Wrong example 2

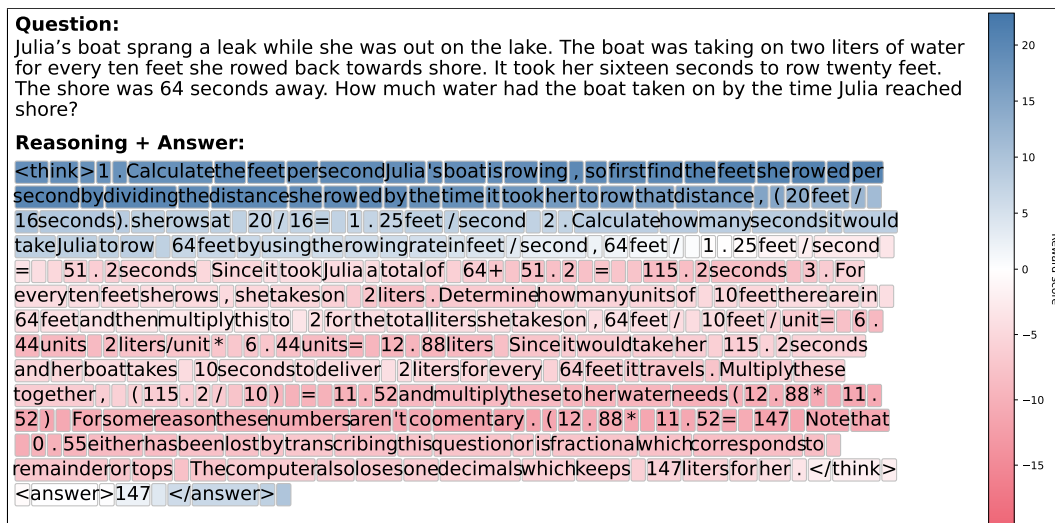
Figure 14: Dense reward illustrations for (Qwen2.5-3B-Instruct & Qwen2.5-1.5B-Instruct). Two correct and two wrong examples of dense rewards ($\gamma = 0.9$). Correct cases show contiguous positive reward bands aligned with decisive reasoning, while wrong cases show inconsistent or negative signals.



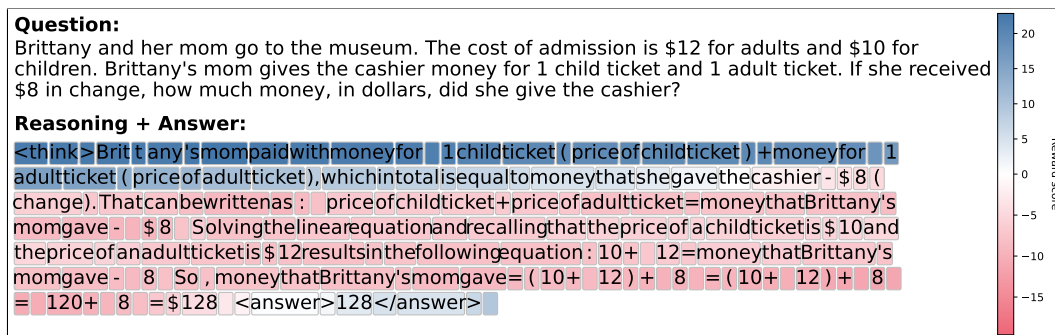
(a) Correct example 1



(b) Correct example 2

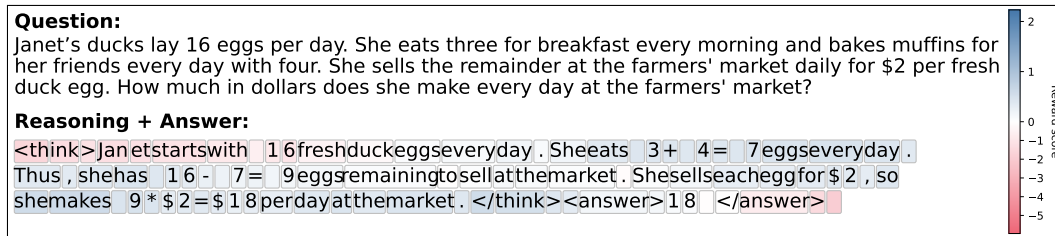


(c) Wrong example 1

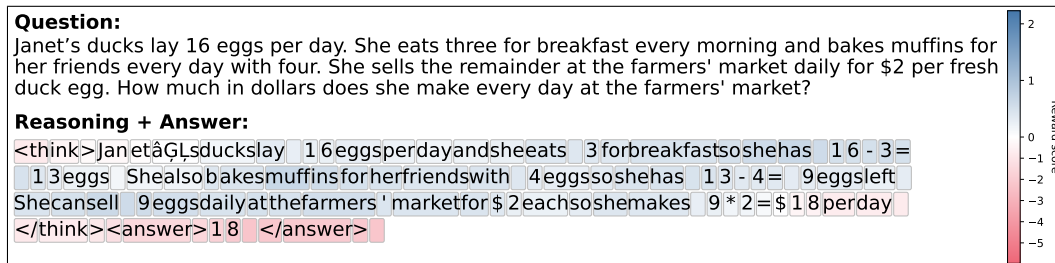


(d) Wrong example 2

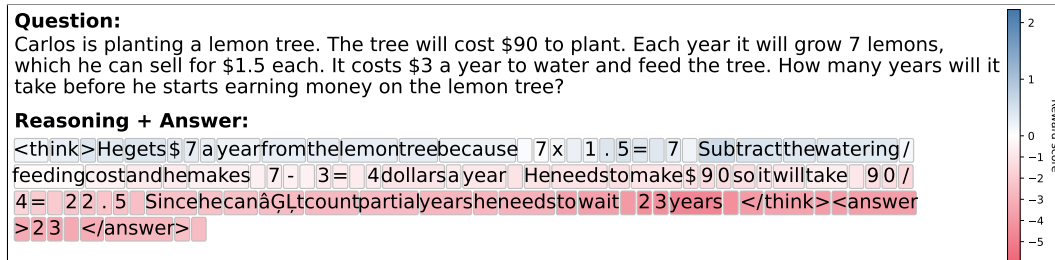
Figure 15: Dense reward illustrations for (Llama3.1-3B-Instruct & Llama3.1-1B-Instruct). Two correct and two wrong examples of dense rewards ($\gamma = 0.9$). Correct cases show contiguous positive reward bands aligned with decisive reasoning, while wrong cases show inconsistent or negative signals.



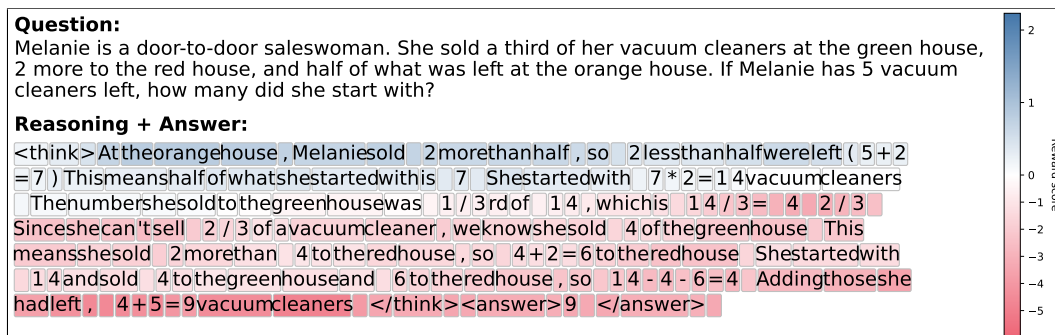
(a) Correct example 1



(b) Correct example 2

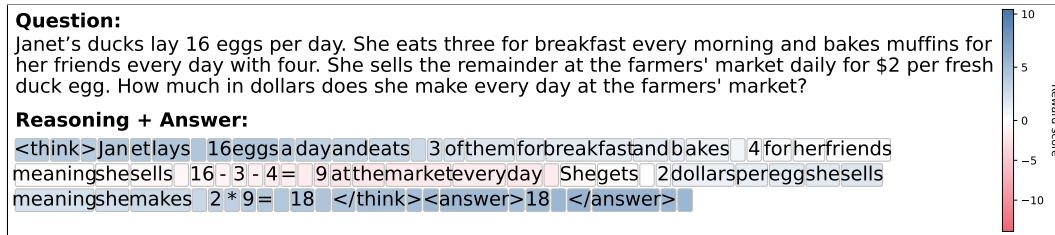


(c) Wrong example 1

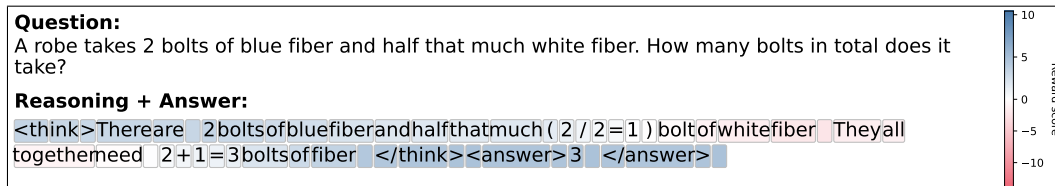


(d) Wrong example 2

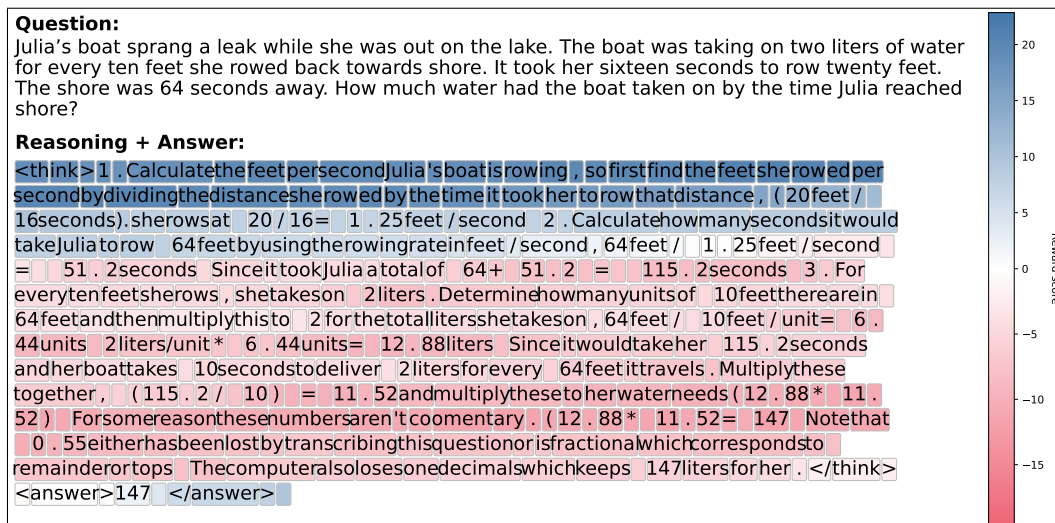
Figure 16: **Dense reward illustrations for (Qwen2.5-7B-Instruct & Qwen2.5-1.5B-Instruct).** Two correct and two wrong examples of dense rewards ($\gamma = 0.9$). Correct cases show contiguous positive reward bands aligned with decisive reasoning, while wrong cases show inconsistent or negative signals.



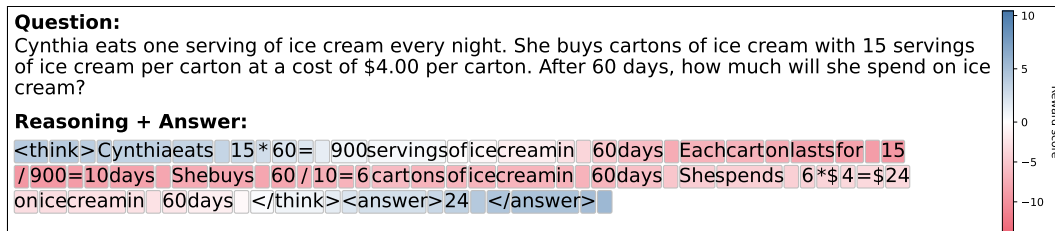
(a) Correct example 1



(b) Correct example 2



(c) Wrong example 1



(d) Wrong example 2

Figure 17: Dense reward illustrations for (Llama3.1-8B-Instruct & Llama3.1-1B-Instruct). Two correct and two wrong examples of dense rewards ($\gamma = 0.9$). Correct cases show contiguous positive reward bands aligned with decisive reasoning, while wrong cases show inconsistent or negative signals.

C ADDITIONAL EXPERIMENTS

C.1 COMAPRISON AGAINST VERIFIABLE REWARDS AND SUPERVISED FINETUNING

We benchmark predictive performance against two references. The first is supervised fine tuning on reasoning traces (SFT). The second is GRPO, which uses a verifiable outcome reward at the final answer and therefore acts as an empirical upper bound. For each backbone, we evaluate the same prompt set and report pass@1, pass@3, pass@5, and pass@10, along with their corresponding confidence intervals. Our method, labelled *Expert Reasoning (ours)*, uses the learned dense reward for training the policy; at test time we decode with the same settings as the baselines.

Table 2 shows consistent trends. GRPO traces the strongest curve across all backbones, as expected from access to verifiable outcomes. Our approach is frequently competitive with SFT and on Qwen2.5-7B it exceeds SFT at all reported pass@k, including pass@1. On Llama3-3B and 8B, as well as on Qwen2.5-3B, our method trails SFT at pass@1 but narrows the gap as k increases. These results quantify the current trade-off between joint optimisation with a learned process reward and outcome supervised training.

Backbone	Algorithm	pass@1	pass@3	pass@5	pass@10
P : Qwen-2.5-3B-Instruct D: Qwen-2.5-0.5B-Instruct	Outcome Sup.	0.80 [0.78, 0.82]	0.90 [0.89, 0.92]	0.93 [0.91, 0.94]	0.95 [0.93, 0.96]
	Exp. Reas. (ours)	0.51 [0.49, 0.53]	0.72 [0.71, 0.74]	0.80 [0.78, 0.81]	0.87 [0.85, 0.88]
	SFT	0.54 [0.53, 0.56]	0.76 [0.75, 0.78]	0.83 [0.81, 0.85]	0.90 [0.88, 0.91]
P: Llama3.1-3B-Instruct D: Llama3.2-1B-Instruct	Outcome Sup.	0.57 [0.55, 0.59]	0.78 [0.77, 0.80]	0.85 [0.83, 0.86]	0.91 [0.89, 0.92]
	Exp. Reas. (ours)	0.32 [0.30, 0.33]	0.53 [0.51, 0.55]	0.63 [0.61, 0.65]	0.75 [0.73, 0.77]
	SFT	0.55 [0.53, 0.57]	0.76 [0.75, 0.78]	0.83 [0.82, 0.85]	0.89 [0.88, 0.91]
P: Qwen-2.5-7B-Instruct D: Qwen-2.5-1.5B-Instruct	Outcome Sup.	0.88 [0.87, 0.90]	0.94 [0.93, 0.95]	0.95 [0.94, 0.96]	0.96 [0.95, 0.97]
	Exp. Reas. (ours)	0.71 [0.69, 0.73]	0.88 [0.87, 0.90]	0.92 [0.91, 0.93]	0.95 [0.94, 0.96]
	SFT	0.67 [0.66, 0.69]	0.87 [0.85, 0.88]	0.91 [0.90, 0.93]	0.95 [0.94, 0.96]
P: Llama3.1-8B-Instruct D: Llama3.2-1B-Instruct	Outcome Sup.	0.73 [0.71, 0.74]	0.88 [0.86, 0.89]	0.91 [0.90, 0.93]	0.94 [0.93, 0.95]
	Exp. Reas. (ours)	0.49 [0.47, 0.51]	0.73 [0.71, 0.75]	0.80 [0.79, 0.82]	0.88 [0.86, 0.89]
	SFT	0.55 [0.53, 0.56]	0.79 [0.78, 0.81]	0.86 [0.84, 0.87]	0.91 [0.90, 0.93]

Table 2: Results (mean \pm CI) for different algorithms across backbones. GRPO serves as the upper bound.

Takeaway: Outcome reward RL with verifiable signals remains the empirical upper bound. The learned process reward is often close to SFT and can exceed it on Qwen 2.5 7B, while trailing on some other settings, especially at pass@1. Closing this gap without losing the training, inference, and diagnostic benefits of the dense reward is a concrete direction for future work.

C.2 CHANGING DISCRIMINATOR BACKBONES

We study the effect of the discriminator backbone size and specialisation for a fixed Qwen2.5-7B Instruct policy. Table 3 shows that a larger general-purpose discriminator (Qwen2.5-1.5B-Instruct) attains the strongest performance across pass@k, with the largest gains at low k. The smaller 0.5B variant trails at pass@1 but approaches parity by pass@10. A maths specialised 1.5B discriminator does not outperform the general purpose counterpart.

Discriminator	pass@1	pass@3	pass@5	pass@10
Qwen 2.5 0.5B Instruct	0.66 [0.65, 0.68]	0.86 [0.84, 0.87]	0.90 [0.89, 0.92]	0.95 [0.93, 0.96]
Qwen 2.5 1.5B Instruct	0.71 [0.69, 0.73]	0.88 [0.87, 0.90]	0.92 [0.91, 0.93]	0.95 [0.94, 0.96]
Qwen 2.5 Math 1.5B Instruct	0.65 [0.64, 0.67]	0.85 [0.84, 0.87]	0.90 [0.89, 0.92]	0.94 [0.93, 0.95]

Table 3: Performance (mean with confidence intervals) for different discriminator backbones with a fixed Qwen2.5-7B-Instruct policy.

Takeaway: A larger general purpose discriminator improves accuracy, especially at pass@1. A maths specialised discriminator of the same size does not confer additional gains in this setting.

C.3 TRAINING WITHOUT PERTURBATION

We study the impact of introducing perturbed traces during training, where we flip operator signs, corrupt numeric literals, and swap the final answer with a previous intermediate quantity. These perturbations are applied to both expert and policy traces and are labelled as non expert. Table 4 and Figure 18 compare training *with* versus *without* perturbations for the Llama3.1-8B-Instruct policy and Llama3.2-1B-Instruct discriminator.

Negative Perturbation	pass@1	pass@3	pass@5	pass@10
✗	0.31 [0.29, 0.32]	0.56 [0.54, 0.57]	0.67 [0.65, 0.69]	0.79 [0.77, 0.80]
✓	0.49 [0.47, 0.51]	0.73 [0.71, 0.75]	0.80 [0.79, 0.82]	0.88 [0.86, 0.89]

Table 4: Results (mean ± CI) when using negative perturbation during training vs. without it for the (Llama3.2-3B-Instruct - Llama3.2-1B-Instruct) combination.

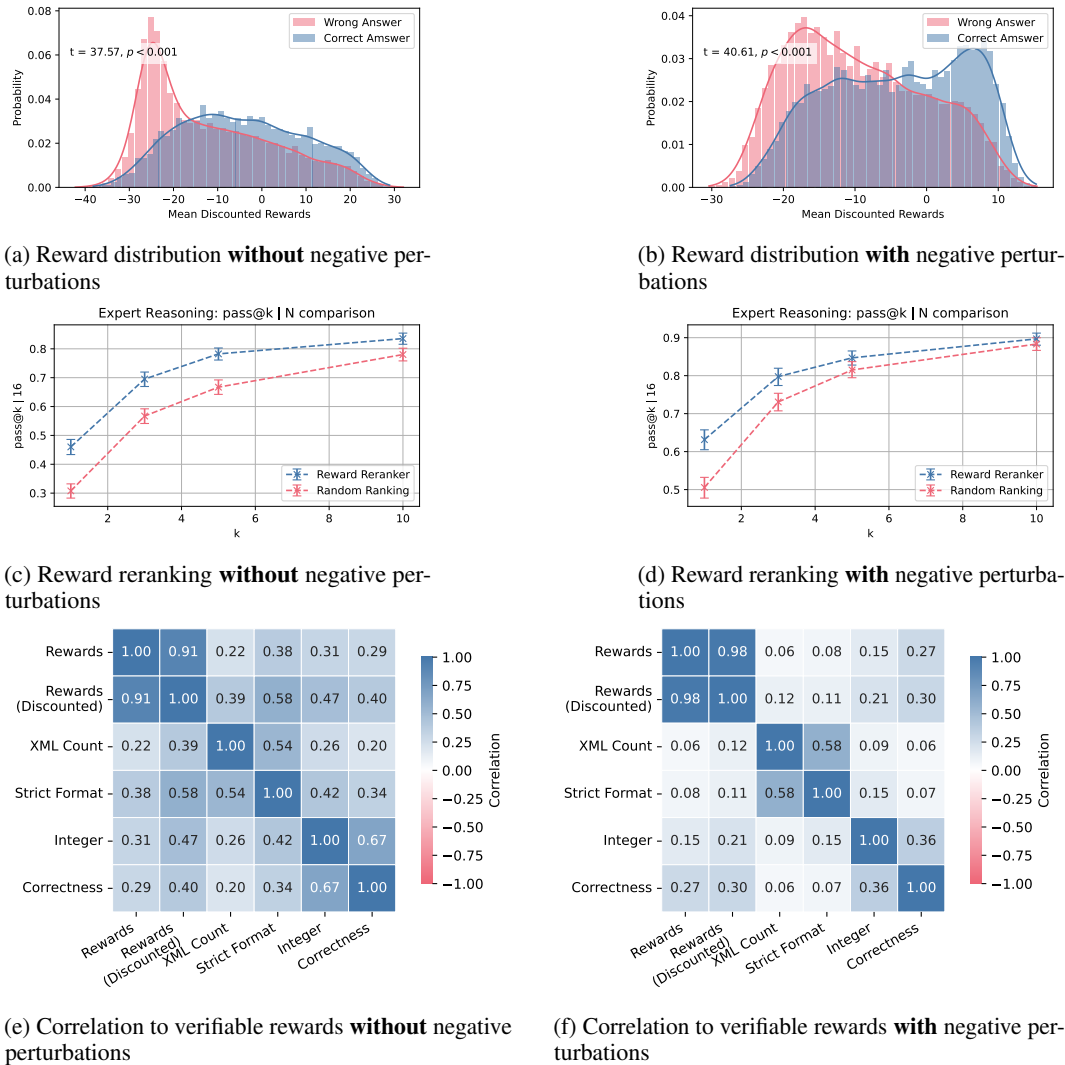


Figure 18: **Distribution and Correlation of Learned Rewards.** For the (Llama3.1-8B-Instruct - Llama3.2-1B-Instruct) combination, we run training with and without negative perturbations.

C.4 WASSERSTEIN GAN DISCRIMINATOR LOSS

We replace the binary cross-entropy objective for the discriminator with a Wasserstein GAN loss and repeat training across backbones. Table 5 and Figures 19, 20, 21, and 22 report predictive performance, reward distributions, and pass@k | N reranking curves. Across settings, the Wasserstein variant yields lower pass@k than binary cross entropy, with the largest drop at pass@1. The learned reward exhibits heavy tails and weaker separation between correct and incorrect answers, which in turn reduces the benefit of reward-guided reranking.

Backbone	Discriminator Loss	pass@1	pass@3	pass@5	pass@10
P: Qwen-2.5-3B-Instruct D: Qwen-2.5-0.5B-Instruct	Binary Cross Entropy Wasserstein GAN	0.51 [0.49, 0.53] 0.58 [0.56, 0.59]	0.72 [0.71, 0.74] 0.75 [0.73, 0.77]	0.80 [0.78, 0.81] 0.81 [0.80, 0.83]	0.87 [0.85, 0.88] 0.88 [0.86, 0.89]
P: Llama3.1-3B-Instruct D: Llama3.2-1B-Instruct	Binary Cross Entropy Wasserstein GAN	0.32 [0.30, 0.33] 0.17 [0.16, 0.18]	0.53 [0.51, 0.55] 0.39 [0.37, 0.40]	0.63 [0.61, 0.65] 0.51 [0.49, 0.53]	0.75 [0.73, 0.77] 0.67 [0.65, 0.69]
P: Qwen-2.5-7B-Instruct D: Qwen-2.5-1.5B-Instruct	Binary Cross Entropy Wasserstein GAN	0.71 [0.69, 0.73] 0.65 [0.64, 0.67]	0.88 [0.87, 0.90] 0.85 [0.84, 0.86]	0.92 [0.91, 0.93] 0.90 [0.89, 0.91]	0.95 [0.94, 0.96] 0.94 [0.93, 0.95]
P: Llama3.1-8B-Instruct D: Llama3.2-1B-Instruct	Binary Cross Entropy Wasserstein GAN	0.49 [0.47, 0.51] 0.33 [0.32, 0.34]	0.73 [0.71, 0.75] 0.59 [0.57, 0.61]	0.80 [0.79, 0.82] 0.70 [0.68, 0.72]	0.88 [0.86, 0.89] 0.81 [0.80, 0.83]

Table 5: Results (mean ± CI) for different algorithms across backbones. GRPO serves as the upper bound.

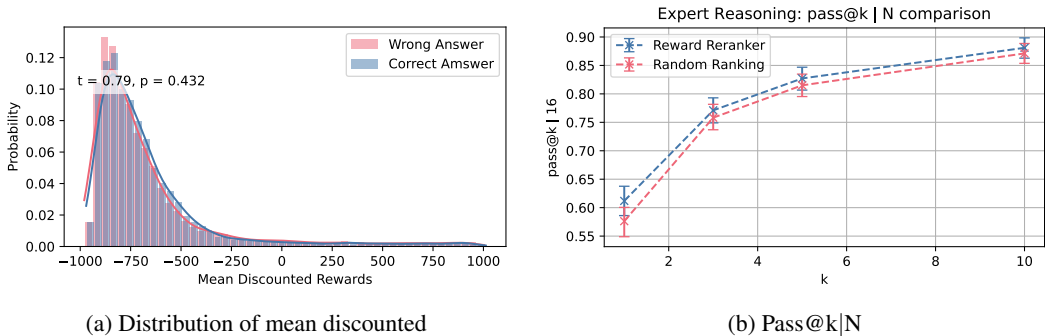


Figure 19: **Benefit of Reasoning Reward Model.** This is for the (Qwen2.5-3B-Instruct - Qwen2.5-0.5B-Instruct) combination using the Wasserstein loss for the discriminator.

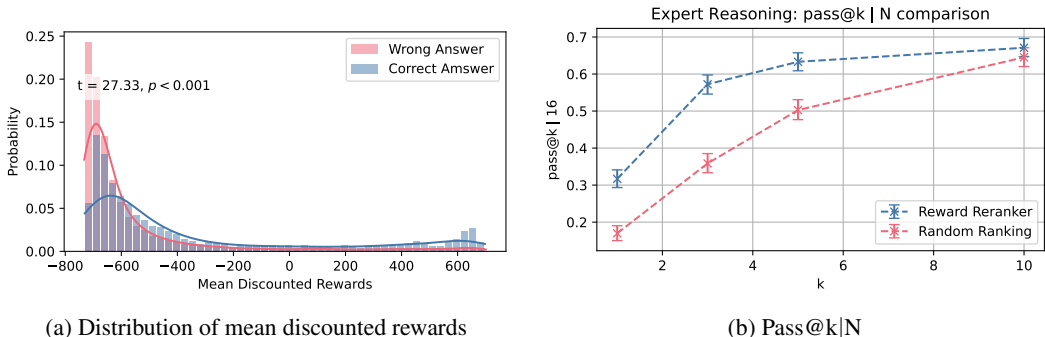


Figure 20: **Benefit of Reasoning Reward Model.** This is for the (Llama3.2-3B-Instruct - Llama3.2-1B-Instruct) combination using the Wasserstein loss for the discriminator.

Takeaway: Binary cross-entropy is a more stable and effective discriminator objective than Wasserstein GAN in our setting. Wasserstein training produces poorly calibrated rewards, weaker class separation, and lower predictive performance.

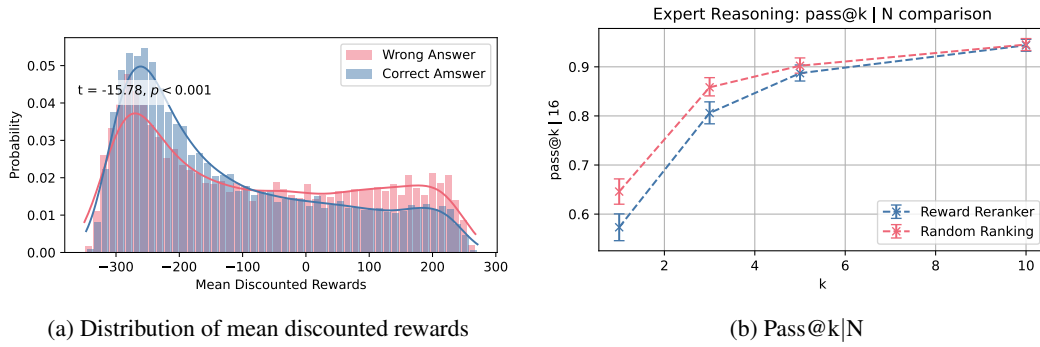


Figure 21: **Benefit of Reasoning Reward Model.** This is for the (Qwen2.5-7B-Instruct - Qwen2.5-1.5B-Instruct) combination using the Wasserstein loss for the discriminator.

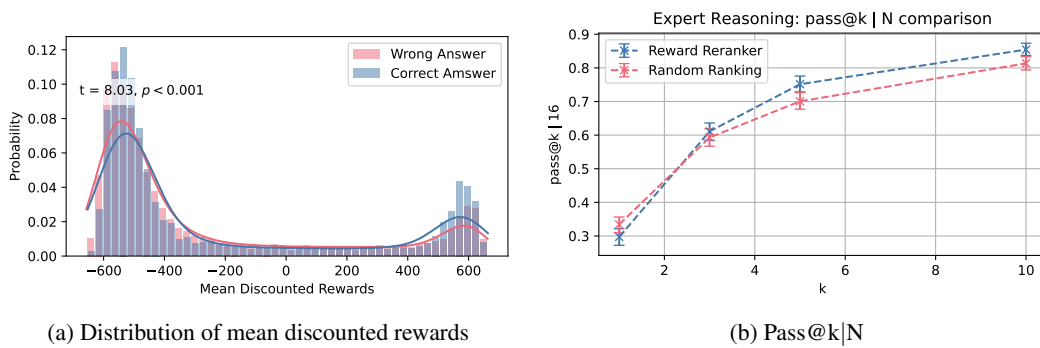


Figure 22: **Benefit of Reasoning Reward Model.** This is for the (Llama3.1-8B-Instruct - Llama3.2-1B-Instruct) combination using the Wasserstein loss for the discriminator.